Received: 6 January 2024 | Revised: 18 February 2024 | Accepted: 19 February 2024

DOI: 10.1002/ardp.202400020

FULL PAPER

ARCH PHARM DPhG
Archiv der Pharmazie

N_1-Benzoylated 5-(4-pyridinyl)indazole-based kinase inhibitors: Attaining haspin and Clk4 selectivity via modulation of the benzoyl substituents

Habiba G. Aboelfotouh[1] | Mennatallah Abdallah[1] | Hend Khalifa[1] | Youssef Aboushady[1] | Ashraf H. Abadi[1] | Matthias Engel[2] | Mohammad Abdel-Halim[1]

[1]Department of Pharmaceutical Chemistry, Faculty of Pharmacy and Biotechnology, German University in Cairo, Cairo, Egypt

[2]Pharmaceutical and Medicinal Chemistry, Saarland University, Saarbrücken, Germany

Correspondence
Mohammad Abdel-Halim, Department of Pharmaceutical Chemistry, Faculty of Pharmacy and Biotechnology, German University in Cairo, Cairo 11835, Egypt.
Email: mohammad.abdel-halim@guc.edu.eg

Matthias Engel, Pharmaceutical and Medicinal Chemistry, Saarland University, Campus C2.3, Saarbrücken D-66123, Germany.
Email: ma.engel@mx.uni-saarland.de

Funding information
None

Abstract

Haspin and Clk4 are both understudied protein kinases (PKs), offering potential targets for the development of new anticancer agents. Thus, the identification of new inhibitors targeting these PKs is of high interest. However, the inhibitors targeting haspin or Clk4 developed to date show a poor selectivity profile over other closely related PKs, increasing the risk of side effects. Herein, we present two newly developed N_1-benzyolated 5-(4-pyridinyl)indazole-based inhibitors (**18** and **19**), derived from a newly identified indazole hit. These inhibitors exhibit an exceptional inhibitory profile toward haspin and/or Clk4. Compound **18** (2-acetyl benzoyl) showed a preference to inhibit Clk4 and haspin over a panel of closely related kinases, with sixfold selectivity for Clk4 (IC_{50} = 0.088 and 0.542 µM, respectively). Compound **19** (4-acetyl benzoyl) showed high selectivity against haspin over the common off-target kinases (Dyrks and Clks) with an IC_{50} of 0.155 µM for haspin. Molecular docking studies explained the remarkable selectivity of **18** and **19**, elucidating how the new scaffold can be modified to toggle between inhibition of haspin or Clk4, despite the high homology of the ATP-binding sites. Their distinguished profile allows these compounds to be marked as interesting chemical probes to assess the selective inhibition of haspin and/or Clk4.

KEYWORDS
anticancer agents, Clk4, haspin, indazole derivatives, kinase inhibitors

Abbreviations: [Pd(dppf)Cl_2], [1,1′- bis(diphenylphosphino)ferrocene]dichloropalladium(II); ADK, adenosine kinase; CDK, cyclin-dependant kinase; CK, casein kinase; CK2 alpha1, casein kinase-2 alpha-1; Clk, Cdc-2 like kinase; CMGC, Cdk, MAPK, GSK, Cdk-like; DCM, dichloromethane; Dyrk, dual-specificity tyrosine-regulated kinase; EDC, 1-ethyl-3-(3-dimethylaminopropyl) carbodiimide; Gsk3β, glycogen synthase kinase β; HIPK1, homodomain-interacting protein kinase-1; PDB, Protein Data Bank; Pim1, proviral integration site for Moloney murine leukemia virus-1; PK, protein kinase; PKC, protein kinase C; ROCK2, Rho associated coiled-coil containing protein kinase 2; RT, room temperature.

1 | INTRODUCTION

Protein kinases (PKs) play a crucial role in cellular signaling and regulation, serving as key modulators of various physiological processes. These enzymes are responsible for the phosphorylation of target proteins, thereby triggering a cascade of molecular events that regulate cellular functions such as growth, differentiation, metabolism, and apoptosis.[1,2] The two largest groups of PKs are serine/threonine kinases and tyrosine kinases.[3] PKs have become the primary focus in the development of anticancer drugs[4] as their deregulation is one the major mechanisms by which cancer cells surpass normal physiological constraints on growth and survival.[5] There are 74 small molecule kinase inhibitor drugs approved by the FDA until May 2023, 65 of them are approved for the management of neoplasms.[6]

Haspin is classified among the atypical serine/threonine kinases as its domain sequence is different from other PKs in the eukaryotic PK super-family.[7,8] Haspin is known to phosphorylate histone H3 at threonine 3[9] and it is responsible for chromosome alignment, centromeric cohesion, and spindle stability during cell division including mitosis and meiosis. It is highly upregulated in a variety of cancer cells such as Burkitt's lymphoma, chronic lymphocytic leukemias, bladder cancer, ovarian cancer, breast cancer and colorectal cancer.[10–13] Inhibition of haspin leads to improper arrangement and separation of sister chromatids during the cell division resulting in an arrest in G2/M phase and subsequently mitotic catastrophe leading to cell apoptosis. Hence, inhibitors targeting haspin exhibit strong antitumor effects.[14] Considering that haspin mainly phosphorylates threonine 3 of histone 3,[15] inhibiting haspin may have fewer side effects compared to other anticancer agents. There are a few reported haspin inhibitors[16] (Figure 1): 5-iodotubercidin which was originally an ADK inhibitor, was the first discovered compound that inhibits haspin along with members of the Clks (Cdc2-like kinases), the Dyrks (dual-specificity tyrosine phosphorylation-regulated kinases), CK1/2, and PKC.[16–19] In addition to the tricyclic fused compounds: LDN-0192960, also co-inhibits Dyrk1A, Dyrk2, Dyrk3, Clk1, and Pim1; LDN-209929 which co-inhibits Dyrk2.[16,20–22] Moreover, the imidazopyridazine derivative CHR-6494 which was found active both in vitro on tumor cells and in vivo in nude mice xenografts of HCT-116 cells, however, the compound displays poor selectivity against other kinases as it co-inhibits Clk1, Dyrk1A, CDK9, GSK3, CK1, CDK5, PIM1, ABL1, and JAK3.[14,20,23] All of these inhibitors lack selectivity for haspin as they cross-react majorly with the Clk family and/or the Dyrk family, both of which belong to the CMGC group of eukaryotic PKs, along with other off-target kinases. Therefore, the development of selective inhibitors that specifically target haspin is necessary to achieve a safe and effective therapeutic effect.

Clk4, a member of the Clk family, is notably one of the least investigated members within this group. Clk family belongs to dual-specificity PKs and is composed of four closely related isoforms: Clk1, Clk2, Clk3, and Clk4. These kinases primarily play a role in alternative

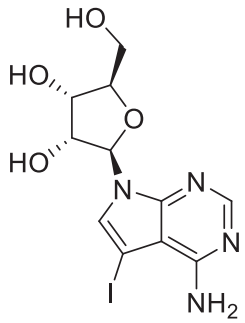

5-Iodotubercidin

Haspin IC_{50}= 0.009 μM

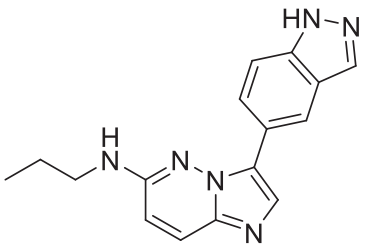

CHR-6494

Haspin IC_{50}= 0.002 μM

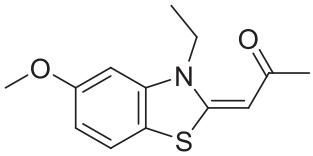

TG003

Clk4 IC_{50} = 0.015 μM
Clk1 IC_{50} = 0.020 μM
Clk2 IC_{50} = 0.200 μM

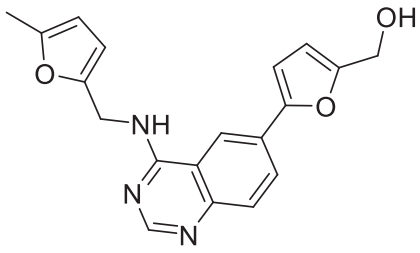

ML167

Clk4 IC_{50} = 0.136 μM
Clk1 IC_{50} = 1.522 μM
Clk2 IC_{50} = 1.648 μM

FIGURE 1 Some examples of reported haspin and Clk1/Clk4 inhibitors.

splicing.[24–26] Clk4 is involved in alternative splicing and RNA processing in Duchenne muscular dystrophy, Alzheimer's disease, HIV-1, influenza virus.[27] Furthermore, its expression is correlated with poor patient survival in triple-negative breast cancer (TNBC) patients, also highly overexpressed in many types of cancer including lung, larynx, colon, rectum, melanomas, glioblastomas, and sarcomas.[26,28,29] Despite the importance of Clk4 in neurodegenerative diseases and cancer, it seems that no selective inhibitors targeting Clk4 have been reported.[24,30] Consequently, the specific functions of Clk4 have remained largely unexplored, as all compounds that were able to exhibit activity against Clk4 were initially designed as Clk1 inhibitors due to their very high sequence similarity in their ATP binding pockets by 100%.[24,31,32] Among prominent Clk1/4 inhibitors are: TG003, CX-4945, T-025, SM08502, indazole1, and several 5-benzothiophene derivatives (Figure 1).[25,30–36] Only ML167 was able to exhibit a superior preference toward Clk4 over the other Clk isoforms.[24,37]

To address this gap, it is essential to focus on the development of selective Clk4 inhibitors. Previous studies have shown that pan inhibition of all four isoforms of Clks leads to significant side effects, including genotoxicity. Therefore, the endeavor to discover specific Clk4 inhibitors holds great promise in understanding the underlying mechanisms of Clk4's involvement in various diseases, particularly cancer.[25,33]

In this study, we describe the development of new haspin and/or Clk4 inhibitors demonstrating high selectivity against the frequently reported and key off-target kinases like the Dyrks and Clk1/2/3.

2 | RESULTS AND DISCUSSION

2.1 | Compound design

An unpublished hit (compound **X**) having N_1-benzoylated 5-pyridin-4-yl-1*H*-indazol-3-yl amine scaffold was identified in our lab during synthesis of PK inhibitors. Compound **X** showed promising effects on haspin (IC_{50} = 0.580 µM) and Clk4 (% inhibition = 45% at 1 µM) (Figure 2) without showing activity on Clk1/2 and Dyrk1A/B (Supporting Information S2: Table S1). In this study, we focused on developing potent and selective haspin and/or Clk4 inhibitors based on compound **X**. Accordingly, we chose some structural modifications on **X** which include monosubstitution of the benzoyl ring by different electron withdrawing and electron donating groups (EDGs) as well as di and tri substitution with different or identical groups at variable positions of the benzoyl. Additionally, in compound **1**, we investigated the optimum position of the pyridine nitrogen.

2.2 | Chemistry

All the planned final compounds were synthesized using a 2-step reaction illustrated in Scheme 1. For compound **1**; the first step is Suzuki-Miyaura cross-coupling reaction between 5-bromo-1*H*-indazol-3-amine and pyridine-3-boronic acid using [Pd(dppf)Cl_2] as a catalyst and Cs_2CO_3 as a base in refluxing dioxane/water overnight to yield compound **A**. Compound **A** was then subjected to an amide coupling reaction with benzoic acid in the presence of EDC as a coupling agent and DMAP as a base in DCM to get compound **1**. Similarity, 5-bromo-1*H*-indazol-3-amine and pyridine-4-boronic acid were coupled to get compound **B**, which was then coupled with different benzoic acid derivatives to yield compounds **2–30**. The methoxy derivatives (**23–24**) were converted to their corresponding hydroxy derivatives (**23a-24a**) by *O*-dealkylation reaction using BBr_3 in dry DCM under cooling (Scheme 2).

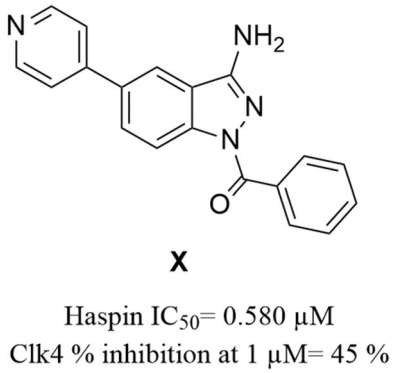

X

Haspin IC_{50}= 0.580 µM
Clk4 % inhibition at 1 µM= 45 %

FIGURE 2 Activity of hit compound **X** on haspin and Clk4.

2.3 | Biological evaluation

2.3.1 | In vitro kinase assay

All of the synthesized compounds were evaluated for their ability to inhibit haspin and Clk4 by screening at 1 µM, IC_{50} values were measured for compounds showing more than 60% inhibition (Table 1).

Structure–activity-relationships (SAR)

Shifting the nitrogen in the 4-pyridyl ring (compound **1**): When we did this modification the activity against haspin and Clk4 was greatly reduced (Table 1). This confirmed the importance of the 4-pyridyl nitrogen and its potential role in binding to the kinase active site (see the docking part). At this point, we decided that the N_1-benzoyl modifications will be explored while adopting the 4-pyridyl indazole scaffold.

Benzoyl monosubstitution with electron withdrawing groups (EWG): Initially, monosubstitution of the phenyl ring with different halogens at *ortho*, *meta* and *para* positions was investigated. Despite their variable size and lipophilicity, the fluorinated (**2–4**), chlorinated (**5–7**), and brominated (**8–10**) analogs exhibited low activity against haspin and Clk4. Interestingly, the *ortho* substitution (compounds **2**, **5**, **8**) showed higher inhibition toward haspin than the respective *meta* and *para* analogs, with *o*-chloro (**5**) showing the highest potency in these analogs against haspin, while *o*-bromo (**8**) showed the highest activity against Clk4. Derivatives with other EWG were further synthesized; incorporating nitro groups at the *ortho* and *meta* positions of phenyl ring yielded compounds **13** and **14**

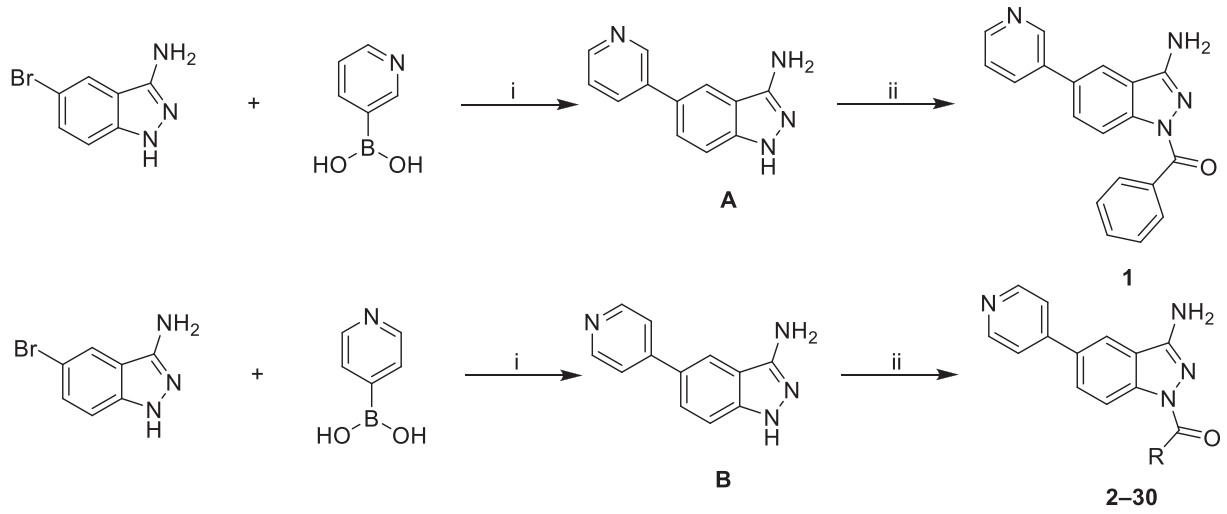

Cpd no.	R	Cpd no.	R
2	2-fluorophenyl	17	4-cyanophenyl
3	3-fluorophenyl	18	2-acetylphenyl
4	4-fluorophenyl	19	4-acetylphenyl
5	2-chlorophenyl	20	2-methylphenyl
6	3-chlorophenyl	21	3-methylphenyl
7	4-chlorophenyl	22	4-methylphenyl
8	2-bromophenyl	23	2-methoxyphenyl
9	3-bromophenyl	24	3-methoxyphenyl
10	4-bromophenyl	25	4-methoxyphenyl
11	3-trifluoromethylphenyl	26	3-hydroxymethylphenyl
12	4-trifluoromethylphenyl	27	3,5-difluorophenyl
13	2-nitrophenyl	28	3,4,5-trifluorophenyl
14	3-nitrophenyl	29	2,4-dichlorophenyl
15	2-cyanophenyl	30	2-hydroxy-4-methoxyphenyl
16	3-cyanophenyl		

SCHEME 1 Synthesis of compounds **1–30**. Reagents and conditions: (i) 2 equiv of Cs_2CO_3, 0.1 equiv of $[Pd(dppf)Cl_2]$ in dioxane/water, reflux at 150°C, 24 h, yield 70%–80%; (ii) 2 equiv of DMAP, 2 equiv of 1-ethyl-3-(3-dimethylaminopropyl) carbodiimide and 2 equiv of the appropriate benzoic acid in dichloromethane, room temperature, overnight, yield 16%–42%.

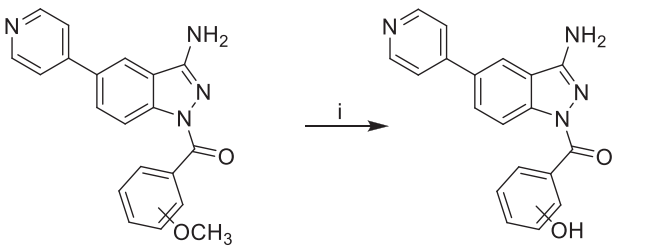

23: 2-methoxyphenyl
24: 3-methoxyphenyl

23a: 2-hydroxyphenyl
24a: 3-hydroxyphenyl

SCHEME 2 Synthesis of compounds **23a–24a**. Reagents and conditions: (i) 5 equiv of 1 M BBr_3 in dichloromethane, room temperature, overnight, yield 18%, and 27%, respectively.

respectively. Likewise, *ortho* substitution (**13**) exhibited higher activity against haspin and Clk4 with an IC_{50} of 0.388 and 0.690 μM respectively, which is more potent than hit compound **X**. However, using the cyano group at the *ortho* position shifted the activity toward Clk4, with compound **15** having an IC_{50} value of 0.615 μM. The *m*- and *p*-cyano (**16** and **17**) showed weak inhibitory activity toward both targets. Trying trifluoromethyl at *meta* and *para* positions in **11** and **12** also showed weak inhibitory activity against both targets. Finally, acetyl substitution at *ortho* position (**18**) was active against haspin with an IC_{50} of 0.542 μM and with a remarkable sixfold higher potency against Clk4 with an IC_{50} value of 0.088 μM. Interestingly, the *para* substitution with the acetyl group (**19**) inverted the profile toward haspin with an IC_{50} of 0.155 μM and the potency against Clk4 was almost abolished.

TABLE 1 Inhibition by the synthesized indazole derivatives.[a]

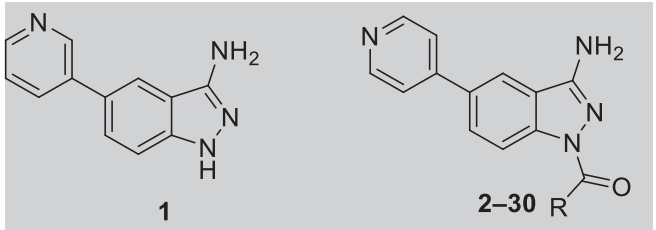

Compound	R	Haspin % Inhibition at 1 μM (IC_{50} [μM])	Clk4 % Inhibition at 1 μM (IC_{50} [μM])
1	-	14	26
2	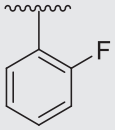	41	34
3	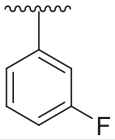	30	12
4	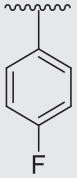	24	3
5	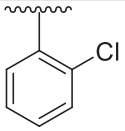	54	40
6	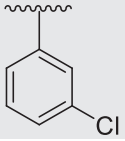	49	30
7	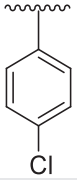	36	51
8	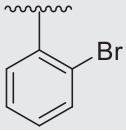	35	56
9	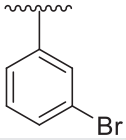	4	18
10	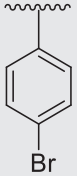	7	11

TABLE 1 (Continued)

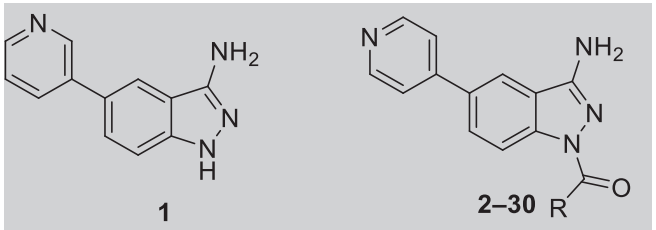

Compound	R	Haspin % Inhibition at 1 μM (IC_{50} [μM])	Clk4 % Inhibition at 1 μM (IC_{50} [μM])
11	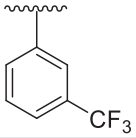	5	22
12	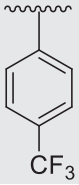	3	14
13	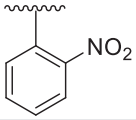	71 (0.388)	62 (0.690)
14	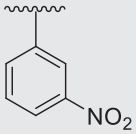	17	22
15	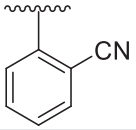	39	60 (0.615)
16	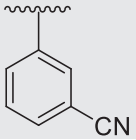	31	18
17	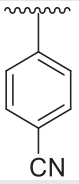	12	19
18	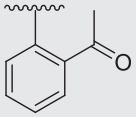	66 (0.542)	93 (0.088)
19	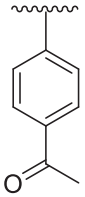	68 (0.155)	14

(Continues)

TABLE 1 (Continued)

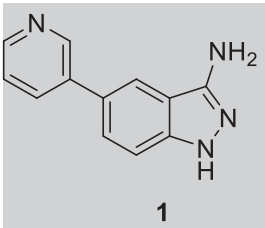

1

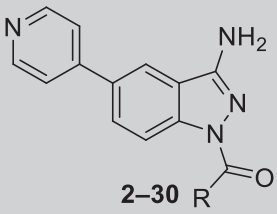

2–30

Compound	R	Haspin % Inhibition at 1 μM (IC_{50} [μM])	Clk4 % Inhibition at 1 μM (IC_{50} [μM])
20	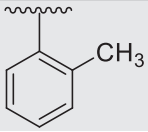	37	24
21	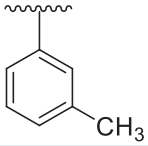	21	45
22	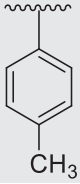	22	34
23	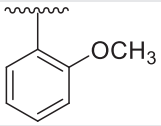	15	31
24	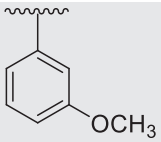	13	8
25	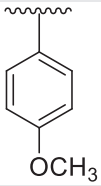	39	28
23a	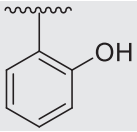	51	81 (0.250)
24a	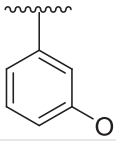	72 (0.478)	51
26	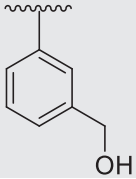	18	31

TABLE 1 (Continued)

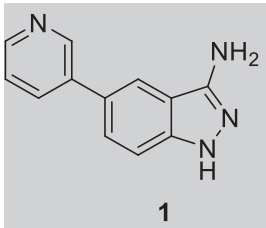

1

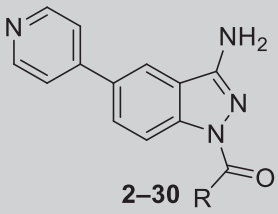

2–30

Compound	R	Haspin % Inhibition at 1 μM (IC_{50} [μM])	Clk4 % Inhibition at 1 μM (IC_{50} [μM])
27	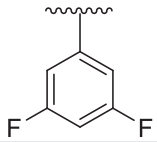	6	17
28	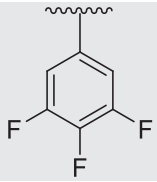	1	5
29	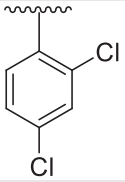	42	21
30	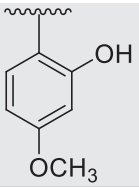	23	49

[a]Reported values represent the means obtained from at least two experiments; standard deviation <10%; the assay was carried out at ATP conc of 25 μM.

Benzoyl monosubstitution with EDG: The use of methyl and methoxy substitution at *ortho*, *meta*, and *para* positions was tried (compounds **20–25**). All of them possessed weak inhibitory activity against the two kinases. Moreover, substitution with hydroxy group at *ortho* and *meta* positions was tried (compounds **23a–24a**). The *o*-OH (**23a**) shifted the potency toward Clk4 with an IC_{50} value of 0.250 μM. However, *m*-OH (**24a**) shifted the activity toward haspin with an IC_{50} of 0.478 μM. Also, substitution with *meta* hydroxymethyl group was tried (**26**) and it showed weak inhibitory activity toward both kinases. Benzoyl di- and trisubstitution of the phenyl ring with different or identical groups at variable positions: We examined the disubstitution with fluoro groups at the three and five positions (**27**) and the 3,4,5-trifluorosubstitution (**28**). Both compounds elicited low activity toward haspin and Clk4. Furthermore, the 2,4-dichloro (compound **29**) also showed reduced activity. Finally, disubstitution with 2–OH–,4–OCH_3 (**30**) displayed a weak activity.

Kinase selectivity profiling

As previously discussed in the introduction, significant inhibition of the Dyrks and the Clks has consistently been observed with the majority of reported inhibitors targeting haspin and Clk4. Accordingly, the most potent compounds on either haspin and/or Clk4 (compounds **18**, **19**, and **23a**) were subjected to an extended selectivity profiling. For this purpose, we employed a carefully selected panel of kinases known for their recurrent co-inhibition by chemically diverse classes of haspin or Clk4 inhibitors (Table 2). Notably, compound **18**, which was sixfold more active against Clk4 than against haspin, did not show significant activity on the tested related kinases except Clk1, however with 11-fold lower potency. Furthermore, compound **19** did not exhibit activity on the tested kinases presented in Table 2 making it the most potent and selective haspin inhibitor in our set of compounds. In addition, in contrast to all previously reported potent inhibitors of Clk4, which demonstrated considerable co-inhibition of the highly homologous Clk1, compound **23a** exhibited an unprecedented level of selectivity over Clk1 as well as the other related kinases.

2.3.2 | Anticancer NCI cell-based screening

As haspin and Clk4 are overexpressed in many cancer cells, compounds that showed activity against haspin and/or Clk4 were screened for their in vitro anticancer activity at the Developmental Therapeutic Program (DTP) of the National Cancer Institute (NCI).[38] The indazole derivatives were examined in vitro at one dose for anticancer activity against total NCI 60 cancer cell line panels that include nine different types of cancers; leukemia, NSC lung cancer, colon cancer, CNS cancer, melanoma, ovarian cancer, renal cancer, prostate cancer, and breast cancer (Supporting Information S2: Table S2). The tested compounds are **X**, **5**, **18**, **19**, **23a**, **24a**. They showed weak inhibitory activity against the tested cell lines, reporting a GI % mean of less than 10% and this can be attributed to different reasons like cell permeability issues or possible plasma protein binding.

TABLE 2 Selectivity profile of **18**, **19**, and **23a** versus frequently reported off-target kinases.[a]

	% Inhibition at 1 µM (IC_{50} [µM])		
Kinase	**Compound 18**	**Compound 19**	**Compound 23a**
Haspin	66 (0.542)	68 (0.155)	51
Clk4	93 (0.088)	14	81 (0.250)
Dyrk1A	16	5	12
Dyrk1B	18	4	3
Dyrk2	30	−1	14
Clk1	50	7	17
Clk2	31	12	13
Clk3	13	8	8
CSNK2A1 (CK2 alpha 1)	7	5	16
GSK3B (GSK3 beta)	2	2	3
HIPK2	3	−1	−1
PIM1	7	−4	10
CDK5/p25	11	4	6
GSK3B	2	16	10

[a]Reported values represent the means obtained from at least two experiments; standard deviation <10%; screening was done at an ATP concentration equivalent to the K_m value of the corresponding enzyme.

2.4 | In silico docking simulation and ADME-Tox profiling

2.4.1 | Prediction of the binding mode by molecular docking

The potential binding modes of the most potent and selective compound on haspin compound **19** (Figure 3), and the most potent compound against Clk4 compound **18** (Figure 4) were analyzed. Our aim was to elucidate the distinct potencies of **19** and **18** using molecular docking. As for **19**, we chose the 3D coordinates of a haspin that were originally cocrystallized with a pyridoquinazoline-based inhibitor as a ligand (PDB entry 7OPS). While for **18**, the 3D coordinates of Clk4 co-crystallized with a naphthyridine-based inhibitor (PDB entry 6FYV) were selected.

Compound **19** was predicted to interact with the ATP-binding site of haspin through multiple CH-π contacts and through key H-bonds with the hinge region and the conserved catalytic lysine residue 511 (Figure 3), creating a basal binding affinity. However, a charge-assisted H-bond with Lys584 (2.49 Å distance) through the *para* acetyl group was also observed, which does not occur in Clk4 (Supporting Information S2: Figure S1), because there is no such lysine. Thus, it can be assumed that this interaction is boosting the binding affinity and selectivity toward haspin. In contrast, the presence of the acetyl group in *ortho* position in **18** failed to reach Lys584 or any other polar residue close by in haspin (Supporting Information S2: Figure S2), thus the binding affinity is reduced when compared with **19**.

On the other hand, **18** was very potent against Clk4, which is also well supported by the docking pose (Figure 4). It makes optimal contacts through several H-bonds and CH–π interaction, enhanced by an additional H-bond of the 2-acetyl group with the backbone NH of Ser247 at the pocket border. Because the 2-acetyl substituent cannot form an equivalent interaction in the ATP pocket of haspin, the additional H-bond might explain the sixfold higher potency of **18** toward Clk4 compared to haspin.

Altogether, the results of our docking study were in full agreement with the observed experimental SAR.

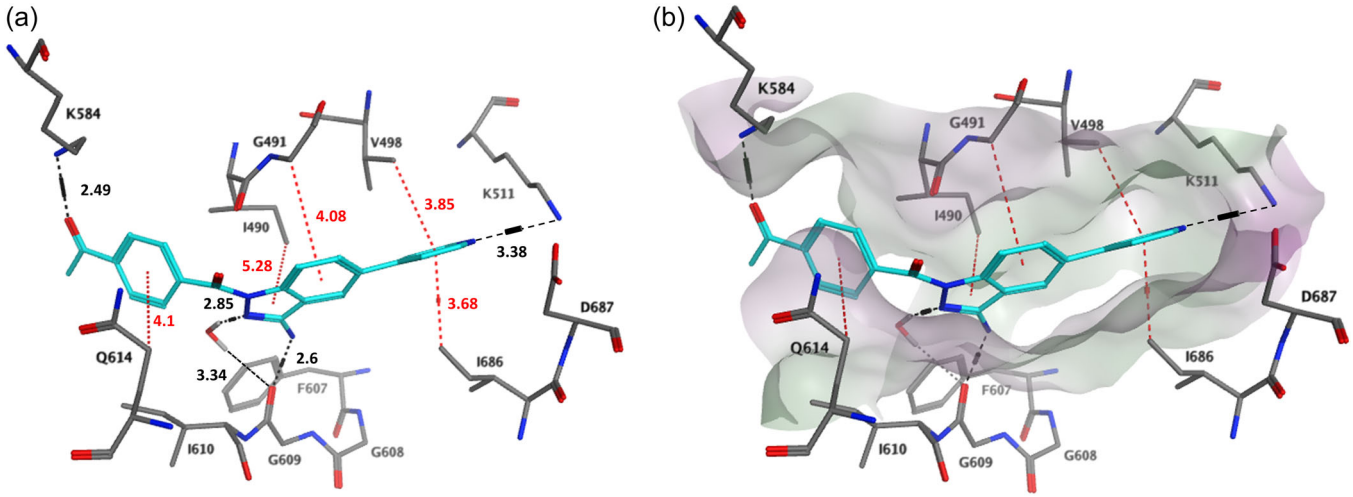

FIGURE 3 Predicted binding mode of compound **19** in the ATP pocket of haspin. Compound **19** docked in the active site of haspin (PDB: 7OPS). Residues interacting directly or indirectly with the ligand are labeled. H-bonds and CH–π interactions are indicated by black and red dotted lines, respectively. (a) In the binding model, **19** is anchored through: a hydrogen bond between the nitrogen of the pyridine ring and the conserved Lys511; another H-bond between the oxygen of the acetyl group and the non conserved Lys584 was observed, in addition to a double H-bond between the Gly609 carbonyl in the hinge region and the primary amine and the imine-like ring nitrogen (bridged by water). CH–π interactions were predicted between the indazole ring and Gly491 and Ile490, respectively, and between the phenyl ring and Gln614. Also, two CH–π interactions were observed between the pyridine ring and Ile686/Val498. (b) In the color code representing the ATP binding pocket surface, green indicates the most lipophilic areas, while magenta highlights the most hydrophilic areas. Some residues in the front were omitted for clarity.

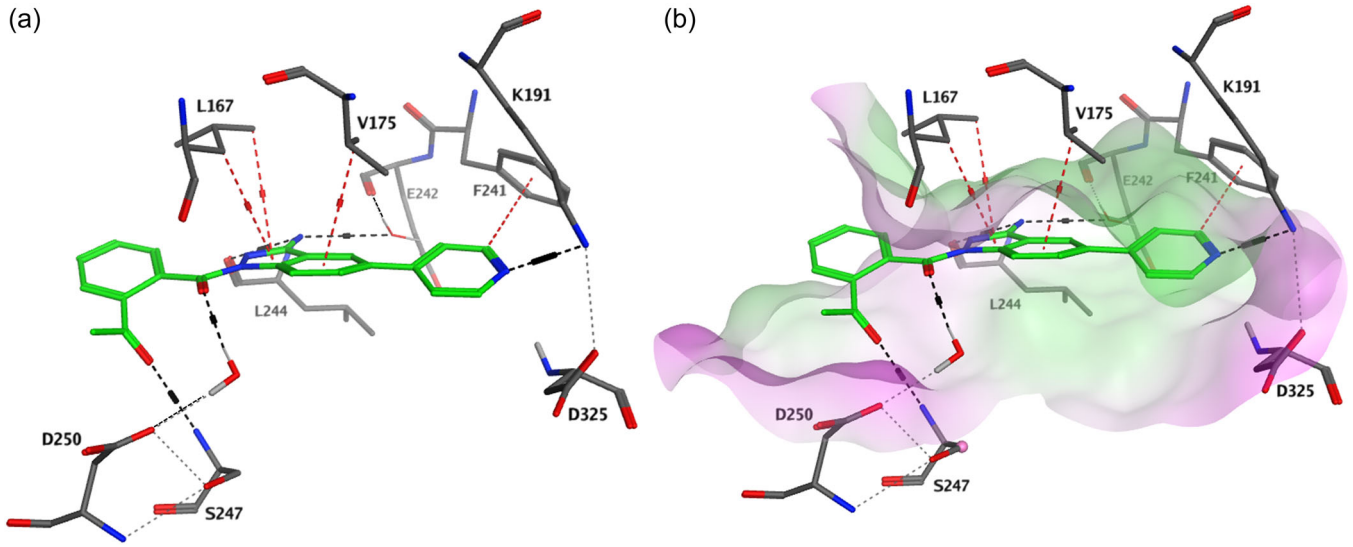

FIGURE 4 Predicted binding mode of compound **18** in the ATP pocket of Clk4. Compound **18** docked in the active site of Clk4 (PDB: 6FYV). Residues interacting directly or indirectly with the ligand are labeled. H-bonds and CH–π interactions are indicated by black and red dotted lines, respectively. (a) In the binding model, **18** is anchored through several H-bonds and CH–π interactions. We detected an H-bond between the nitrogen of the pyridine ring and the conserved Lys191, another one was observed between the amine group and the Leu244 backbone. Water-mediated H-bonds were observed between the carbonyl group and Asp250 as well as between the amine group and Glu242. In addition to an another H-bond between the 2-acetyl group and the backbone NH of Ser247. Double CH–π interactions were detected between the indazole ring and Leu167 as well as another one between the indazole ring and Val175, in addition to another CH-π interaction between the pyridine ring and Phe241. (b) In the color code representing the ATP binding pocket surface, green indicates the most lipophilic areas, while magenta highlights the most hydrophilic areas. Some residues in the front were omitted for clarity.

TABLE 3 Physicochemical descriptors and predicted ADME properties of active compounds.

Compound	F-Csp3	HBA	HBD	MR	TPSA	XLOGP3	logS	log K_p	Bioavailability score
X	0	3	1	93.54	73.8	3.32	−4.33	−5.86	0.55
13	0	5	1	102.36	119.62	3.15	−4.36	−6.26	0.55
15	0	4	1	98.25	97.59	3.04	−4.26	−6.21	0.55
18	0.05	4	1	103.73	90.87	3	−4.25	−6.34	0.55
19	0.05	4	1	103.73	90.87	3	−4.25	−6.34	0.55
23a	0	4	2	95.56	94.03	3.52	−4.53	−5.82	0.55
24a	0	4	2	95.56	94.03	2.96	−4.18	−6.21	0.55

Abbreviations: F-Csp3, the fraction of sp^3-hybridized carbon atoms; HBA, the number of hydrogen bond acceptors; HBD, the number of hydrogen bond donors; logS, solubility estimate and log K_p (cm/s): skin permeation estimate; MR, molar refractivity; TPSA, topological polar surface area; XLOGP3, lipophilicity estimate.

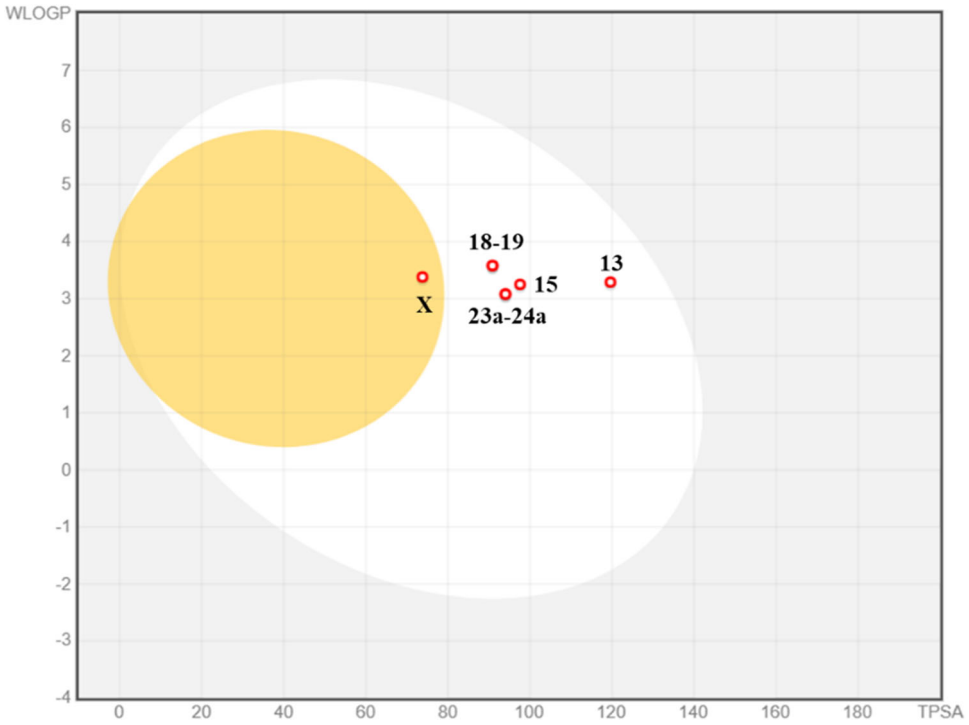

FIGURE 5 BOILED-Egg representation for the predicted blood–brain barrier penetration (egg-yolk area), and human intestinal absorption (egg area) of synthesized molecules **X**, **13**, **15**, **18**, **19**, **23a**, and **24a**.

2.4.2 | ADME-Tox profiling through the SWISSADME online platform

The physicochemical properties, human intestinal absorption (HIA), blood–brain barrier (BBB) penetration, drug-likeness, and medicinal chemistry properties of the active compounds **X**, **13**, **15**, **18**, **19**, **23a**, and **24a** were assessed using SwissADME online tool.[39] The results are shown in Table 3 and Figure 5.

According to the in silico ADME results, all compounds possessed drug-like candidate qualities and did not violate any of the drug-likeness requirements. All compounds are predicted to have high to moderate water solubility, as indicated by the logS value higher than −6 (LogS should be in the range from −0.6 to +6.0).[39] All derivatives are predicted to have high gastrointestinal absorption with an oral bioavailability score of 0.55. All derivatives are drug-like with zero rule violation, according to the Lipinski, Ghose, Veber, Muegge, and Egan rules. None of the derivatives gave any alerts in the pan-assay interference compounds (PAINS) filter. One Brenk structural alert (**13**) for all molecules was returned in calculation, having a nitro group and possessing heteroatoms (N and O) outside a ring.[40] The polarity estimate, topological polar surface area (TPSA) lays between the accepted

range (20–130 Å^2). The lipophilicity estimate, XLOGP3 was in the acceptable range between −0.7 and +6.0.[39,41]

To predict the passive human gastrointestinal absorption and brain access of our molecules, the BOILED-Egg (Brain Or IntestinaL EstimateD permeation predictive model) plot of WLOGP (the log P method developed by Wildman and Crippen)[39] versus TPSA was retrieved from the Swiss-ADME platform for **X**, **13**, **15**, **18**, **19**, **23a**, and **24a** (Figure 2). The BOILED-Egg analysis indicates that all derivatives fell within the permissible range of standard drugs. All derivatives are predicted to fill within the white area of the egg, indicating good human intestinal absorption. Only compound **X** laid in the yellow egg yolk area, which indicate that it has also BBB permeability (white and yolk areas are not mutually exclusive).[42]

3 | CONCLUSIONS

In the present study, novel indazole derivatives were synthesized as haspin/Clk4 inhibitors. Out of these compounds, compound **19** was the most potent against haspin with IC_{50} = 0.155 µM and exhibited unprecedented selectivity over the tested related and common off-target kinases like Clk and Dyrk kinases. Therefore, compound **19** was identified as a new lead structure for the development of selective haspin inhibitors; these are needed to evaluate the impact of selective haspin inhibition in diverse diseases. Compounds which carry *ortho* oxygenated substituents (acetyl and hydroxy) could show preferential inhibition for Clk4: compounds **18** (IC_{50} = 0.088 µM) and **23a** (IC_{50} = 0.250 µM), respectively. **18** displayed a sixfold lower inhibition of haspin as an off-target. Compound **23a** showed interesting selectivity for Clk4 versus other Clk isoforms. These results indicate that the new scaffold is also suitable for the development of probe compounds for the selective inhibition of Clk4 in disease models. In contrast to the more studies Clk1-3 isoforms, little is known regarding the pathogenic roles of Clk4 in cancer and further disorders that show aberrant pre-mRNA splicing.[24,43]

Altogether, a new scaffold with a benzamide extension was discovered, which is placed at a favorable position in the binding site where it is able to target non conserved residues at the border of the ATP binding pocket. This allowed us to modulate the inhibitory profile of benzamide derivatives toward the frequently co-inhibited kinases haspin and Clk4 through suitable substituents. While a basal binding affinity of the scaffold seems to be created by interactions in the ATP binding pocket, the experimental SAR together with the docking results clearly suggest that a strong potency against either of the target kinases strongly depends on additional interactions of substituents at the benzamide moiety. Since the latter interactions concern amino acid residues that are non conserved between Clk4, haspin and related kinases, this particular property of the scaffold is prerequisite to achieve selectivity within the Clk family of kinases and haspin, which all possess ATP binding pockets lined by mostly identical amino acid residues.

4 | EXPERIMENTAL

4.1 | Chemistry

4.1.1 | General

All solvents and reagents used were obtained from commercial suppliers and were used without further purification. The solvents used in chemical synthesis were of HPLC grade. Purification of intermediates and products was carried out using column chromatography using silica gel 60 (40–63 µM). Reaction progress was monitored by TLC using fluorescent precoated silica gel plates and detection of the components was made by short UV light (λ = 254 nm). All final compounds had a percentage purity of at least 95%, and this could be verified by means of HPLC coupled with mass spectrometry. Mass spectrometric analysis (UHPLC-ESI-MS) was performed using the Waters ACQUITY Xevo TQD system, which consisted of an ACQUITY UPLC H-Class system and Xevo™ TQD triple-quadrupole tandem mass spectrometer with an electrospray ionization (ESI) interface (Waters Corp.). Acquity BEH C18 100 × 2.1 mm column (particle size, 1.7 µm) was used to separate analytes (Waters). The solvent system consisted of water containing 0.1% formic acid (A) and 0.1% formic acid in acetonitrile (B). HPLC method: flow rate 200 µL/min. The percentage of B started at an initial of 5% and maintained for 1 min, then increased up to 100% during 10 min, kept at 100% for 2 min, and flushed back to 5% in 3 min then kept at 5% for 1 min. The MS scan was carried out at the following conditions: capillary voltage 3.5 kV, cone voltage 20 V, radio frequency (RF) lens voltage 2.5 V, source temperature 150°C and desolvation gas temperature 500°C. Nitrogen was used as the desolvation and cone gas at a flow rate of 1000 and 20 L/h, respectively. System operation and data acquisition were controlled using Mass Lynx 4.1 software (Waters). HRMS was performed as previously reported in ElHady et al.[44] NMR data (see the Supporting Information) were recorded using a Bruker Avance Neo 500 MHz (^{1}H at 500.0 MHz; ^{13}C at 126.0 MHz), equipped with a Prodigy Cryo-probe. The chemical shifts are referenced to the residual protonated solvent signals.

The InChI codes of the investigated compounds, together with some biological activity data, are provided as Supporting Information.

4.1.2 | Procedure A, procedure for the synthesis of 5-(pyridin-3-yl)-1*H*-indazol-3-amine (**A**)

A stirred mixture of 5-bromo-1*H*-indazol-3-amine (2.5 mmol, 1 equiv), pyridine-3-boronic acid (10 mmol, 4 equiv), cesium carbonate (10 mmol, 4 equiv), and [Pd(dppf)Cl_2] (0. 25 mmol, 0.1 equiv) in 60 mL dioxane and 15 mL water was refluxed at 150°C for 24 h. After completion, the solvent was removed under vacuum and the residue was partitioned between ethyl acetate (50 mL) and brine solution (30 mL). Then, re-extraction of the aqueous layer using ethyl acetate (4 × 50 mL) was performed, and the organic layers were combined and dried over anhydrous $MgSO_4$ and evaporated under reduced pressure. This was followed by purification of the desired compound **A** using recrystallization by adding hot dichloromethane to reach

complete dissolution, then hexane was added till the solution showed persistent turbidity. The mixture was left to cool at 0°C for 10 min. The pure 1*H*-indazol-3-amine derivative was obtained as a faint brown powder in a yield of 80%; mp 200–204°C; ^{1}H NMR 500 MHz, DMSO-d_6) δ 11.55 (s, 1H), 8.93 (s, 1H), 8.51 (d, J = 4.0 Hz, 1H), 8.11 (s, 1H), 8.04 (d, J = 7.8 Hz, 1H), 7.61 (d, J = 8.5 Hz, 1H), 7.47 (dd, J = 7.5, 4.8 Hz, 1H), 7.35 (d, J = 8.6 Hz, 1H), 5.48 (s, 2H); ^{13}C NMR (126 MHz, DMSO-d_6) δ 150.20, 147.83, 141.48, 136.95, 134.03, 126.92, 125.77, 124.30, 119.28, 115.25, 110.61; (ESI-MS) m/z = 211.09 $[M+H]^+$.

4.1.3 | Procedure B, procedure for the amide coupling reaction to give compound **1** using compound **A**

A mixture of the 1*H*-indazol-3-amine derivative (**A**) (0.5 mmol, 1 equiv), unsubstituted benzoic acid (1 mmol, 2 equiv), 4-dimethylaminopyridine (1 mmol, 2 equiv), and 1-ethyl-3-(3-dimethylaminopropyl) carbodiimide (1 mmol, 2 equiv) was stirred in 50 mL dichloromethane overnight at room temperature. Afterwards, the mixture was concentrated under vacuum, water was added and then extracted using dichloromethane (1 × 50 mL). The organic layer was collected, dried over anhydrous $MgSO_4$ and evaporated under reduced pressure. This was followed by purification of compound **1** using CC. Compound **1** was obtained as a white powder in a yield of 75%; mp 200–204°C; ^{1}H NMR (500 MHz, DMSO-d_6) δ 8.97 (d, J = 1.7 Hz, 1H), 8.61 (d, J = 3.7 Hz, 1H), 8.45 (d, J = 8.6 Hz, 1H), 8.36 (d, J = 1.0 Hz, 1H), 8.17–8.12 (m, 1H), 8.02–7.99 (m, 1H), 7.98–7.95 (m, 2H), 7.55 (ddd, J = 17.6, 14.6, 7.3 Hz, 4H), 6.60 (s, 2H); ^{13}C NMR (126 MHz, DMSO-d_6) δ 166.50, 153.47, 148.53, 147.68, 139.82, 135.19, 134.28, 134.13, 133.12, 131.23, 130.05, 128.67, 127.74, 123.98, 121.13, 119.11, 116.24. (ESI-MS) m/z = 315.12 $[M+H]^+$. HRMS (ESI+) m/z calcd. for $C_{19}H_{15}N_4O^+$ $[M+H]^+$: 315.1240 found 315.1237.

4.1.4 | Procedure C, procedure for the synthesis of 5-(pyridine-4-yl)-1*H*-indazol-3-amine (**B**)

A stirred mixture of 5-bromo-1*H*-indazol-3-amine (2.5 mmol, 1 equiv), pyridine-4-boronic acid (10 mmol,4 equiv), cesium carbonate (10 mmol, 4 equiv), and $[Pd(dppf)Cl_2]$ (0.25 mmol, 0.1 equiv) in 60 mL dioxane and 15 mL water was refluxed at 150°C for 24 h. When finished, the solvent was removed under vacuum and the residue was partitioned between ethyl acetate (50 mL) and brine solution (30 mL). Extraction was then done using ethyl acetate (4 × 50 mL) and the combined organic layers were dried over anhydrous $MgSO_4$ and evaporated under reduced pressure. This was followed by purification of the desired compound **B** using recrystallization by adding hot dichloromethane to reach complete dissolution, then hexane was added till the solution showed persistent turbidity. The mixture was left to cool at 0°C for 10 min. The pure 1*H*-indazol-3-amine derivative was obtained as a brown powder in a yield of 70%–80% and used in the next step without further purification; mp 190–191°C; ^{1}H NMR (500 MHz, DMSO-d_6) δ 11.61 (s, 1H), 8.60 (d, J = 4.0 Hz, 2H), 8.26 (s, 1H), 7.72–7.66 (m, 3H), 7.35 (d, J = 8.7 Hz, 1H), 5.55 (s, 2H); ^{13}C NMR (126 MHz, DMSO-d_6) δ 150.55, 150.46, 148.26, 141.96, 126.80, 125.43, 121.10, 119.69, 115.23, 110.60; (ESI-MS) m/z = 211.09 $[M+H]^+$.

4.1.5 | Procedure D, general procedure for the amide coupling reaction to give compounds **2**–**30** using compound **B**

A mixture of the 1*H*-indazol-3-amine derivative (**B**) (0.5 mmol, 1 equiv), the appropriate benzoic acid (1 mmol, 2 equiv), 4-dimethylaminopyridine (1 mmol, 2 equiv), and 1-ethyl-3-(3-dimethylaminopropyl) carbodiimide (1 mmol, 2 equiv) was stirred in 50 mL dichloromethane overnight at room temperature. Afterward, the solvent was removed under vacuum, water was added, and the aqueous layer was extracted using dichloromethane (1 × 50 mL). The organic layer was collected, dried over anhydrous $MgSO_4$ and evaporated under reduced pressure. This was followed by purification of the final compounds using CC.

[3-Amino-5-(pyridin-4-yl)-1*H*-indazol-1-yl]-(2-fluorophenyl) methanone (**2**): The title compound was prepared following procedure D using 2-fluorobenzoic acid to give a yellow solid: yield (39%). The product was purified by CC (DCM/MeOH 95:5); mp 175–176°C; ^{1}H NMR (500 MHz, DMSO-d_6) δ 8.87 (t, J = 9.1 Hz, 2H), 8.61 (s, 1H), 8.52 (d, J = 8.5 Hz, 1H), 8.26 (dd, J = 9.0, 7.5 Hz, 1H), 8.05 (d, J = 5.5 Hz, 2H), 7.73 (dd, J = 10.5, 3.5 Hz, 1H), 7.66 (dd, J = 13.9, 5.7 Hz, 1H), 7.45–7.40 (m, 2H), 6.77 (s, 2H); ^{13}C NMR (126 MHz, acetone-d_6) δ 163.95, 159.40 (d, $^1J_{C-F}$ = 283.8 Hz), 153.25, 147.70, 140.65, 133.31, 132.21 (d, $^3J_{C-F}$ = 8.2 Hz), 130.02 (d, $^4J_{C-F}$ = 2.6 Hz), 128.85, 123.97 (d, $^3J_{C-F}$ = 3.5 Hz), 122.81, 122.31, 121.63, 120.64, 119.63, 116.24, 115.53 (d, $^2J_{C-F}$ = 21.4 Hz); (ESI-MS) m/z = 333.3 $[M+H]^+$. HRMS (ESI+) m/z calcd. for $C_{19}H_{14}FN_4O^+$ $[M+H]^+$: 333.1146 found 333.1143 4.2.7.

[3-Amino-5-(pyridin-4-yl)-1*H*-indazol-1-yl]-(3-fluorophenyl) methanone (**3**): The title compound was prepared following procedure D using 3-fluorobenzoic acid to give a white solid: yield (42%). The product was purified by CC (DCM/MeOH 95:5); mp 180–181°C; ^{1}H NMR (500 MHz, acetone-d_6) δ 8.55 (dd, J = 4.6, 1.4 Hz, 2H), 8.44 (d, J = 8.6 Hz, 1H), 8.27 (d, J = 1.5 Hz, 1H), 7.95 (dd, J = 8.6, 1.7 Hz, 1H), 7.82–7.77 (m, 2H), 7.62 (dd, J = 4.6, 1.5 Hz, 2H), 7.47–7.42 (m, 1H), 7.28–7.23 (m, 1H), 5.97 (s, 2H); ^{13}C NMR (126 MHz, acetone-d_6) δ 165.87, 162.68 (d, $^1J_{C-F}$ = 243.6 Hz), 154.28, 151.37, 148.05, 142.06,137.47 (d, $^3J_{C-F}$ = 7.2 Hz), 135.11, 130.54 (d, $^3J_{C-F}$ = 8.0 Hz), 129.48, 127.51 (d, $^4J_{C-F}$ = 2.6 Hz), 122.24, 121.98, 119.77, 119.02 (d, $^2J_{C-F}$ = 21.2 Hz), 118.45 (d, $^2J_{C-F}$ = 24.0 Hz), 117.56; (ESI-MS) m/z = 333.3 $[M+H]^+$. HRMS (ESI+) m/z calcd. for $C_{19}H_{14}FN_4O^+$ $[M+H]^+$: 333.1146 found 333.1145.

[3-Amino-5-(pyridin-4-yl)-1*H*-indazol-1-yl]-(4-fluorophenyl) methanone (**4**): The title compound was prepared following procedure D using 4-fluorobenzoic acid to give a yellow solid: yield (38%). The product was purified by CC (DCM/MeOH 95:5); mp 169–170°C; ^{1}H NMR (500 MHz, DMSO-d_6) δ 8.73–8.68 (m, 2H), 8.47 (dd, J = 8.8,

5.0 Hz, 2H), 8.15–8.08 (m, 3H), 7.77 (dd, *J* = 4.6, 1.5 Hz, 2H), 7.40–7.35 (m, 2H), 6.67 (s, 2H); ^{13}C NMR (126 MHz, DMSO-d_6) δ 165.58, 164.30 (d, $^{1}J_{C-F}$ = 249.9 Hz), 153.89, 150.86, 146.96, 140.96, 133.59 (d, $^{3}J_{C-F}$ = 9.3 Hz), 130.98 (d, $^{4}J_{C-F}$ = 2.9 Hz), 129.04, 121.63, 121.50, 119.84, 116.71, 115.30 (d, $^{2}J_{C-F}$ = 21.6 Hz); (ESI-MS) *m/z* = 333.3 $[M+H]^+$. HRMS (ESI+) *m/z* calcd. for $C_{19}H_{14}FN_4O^+$ $[M+H]^+$: 333.1146 found 333.1144.

[3-Amino-5-(pyridin-4-yl)-1*H*-indazol-1-yl]-(2-chlorophenyl) methanone (**5**): The title compound was prepared following procedure D using 2-chlorobenzoic acid to give a yellow solid: yield (17%). The product was purified by CC (DCM/MeOH 95:5); mp 188–189°C; ^{1}H NMR (500 MHz, DMSO-d_6) δ 8.72–8.67 (m, 2H), 8.46 (d, *J* = 9.4 Hz, 2H), 8.11 (d, *J* = 9.0 Hz, 1H), 7.77 (dd, *J* = 4.6, 1.6 Hz, 2H), 7.62 (d, *J* = 7.4 Hz, 1H), 7.57 (d, *J* = 7.7 Hz, 1H), 7.52 (td, *J* = 7.7, 1.6 Hz, 1H), 7.49–7.45 (m, 1H), 6.70 (s, 2H); ^{13}C NMR (126 MHz, DMSO-d_6) δ 167.25, 154.19, 150.87, 146.95, 139.91, 136.34, 132.94, 131.97, 131.21, 131.04, 130.25, 129.64, 129.26, 127.68, 122.15, 121.70, 120.01; (ESI-MS) *m/z* = 349.12 $[M+H]^+$, 351.12 $[M+2+H]^+$. HRMS (ESI+) *m/z* calcd. for $C_{19}H_{14}ClN_4O^+$ $[M+H]^+$: 349.0851 found 349.0849.

[3-Amino-5-(pyridin-4-yl)-1*H*-indazol-1-yl]-(3-chlorophenyl) methanone (**6**): The title compound was prepared following procedure D using 3-chlorobenzoic acid to give a white solid: yield (35%). The product was purified by CC (DCM/MeOH 95:5); mp 191–192°C; ^{1}H NMR (500 MHz, DMSO-d_6) δ 8.70 (d, *J* = 5.9 Hz, 2H), 8.47 (dd, *J* = 13.3, 4.8 Hz, 2H), 8.10 (dd, *J* = 8.6, 1.6 Hz, 1H), 8.03 (s, 1H), 7.92 (d, *J* = 7.7 Hz, 1H), 7.77 (d, *J* = 6.0 Hz, 2H), 7.70–7.65 (m, 1H), 7.57 (t, *J* = 7.9 Hz, 1H), 6.72 (s, 2H); ^{13}C NMR (126 MHz, DMSO-d_6) δ 165.23, 154.06, 150.85, 146.93, 140.81, 136.69, 133.83, 132.89, 131.55, 130.31, 130.17, 129.11, 129.09, 121.71, 121.64, 119.88, 116.69; (ESI-MS) *m/z* = 349.12 $[M+H]^+$, 351.12 $[M+2+H]^+$. HRMS (ESI+) *m/z* calcd. for $C_{19}H_{14}ClN_4O^+$ $[M+H]^+$: 349.0851 found 349.0848.

[3-Amino-5-(pyridin-4-yl)-1*H*-indazol-1-yl)]-(4-chlorophenyl) methanone (**7**): The title compound was prepared following procedure D using 4-chlorobenzoic acid to give a white solid: yield (32%). The product was purified by CC (DCM/MeOH 95:5); mp 185–186°C; ^{1}H NMR (500 MHz, DMSO-d_6) δ 8.70 (dd, *J* = 4.6, 1.5 Hz, 2H), 8.46 (dd, *J* = 11.1, 5.0 Hz, 2H), 8.09 (dd, *J* = 8.7, 1.7 Hz, 1H), 8.05–8.01 (m, 2H), 7.77 (dd, *J* = 4.6, 1.6 Hz, 2H), 7.64–7.60 (m, 2H), 6.68 (s, 2H); ^{13}C NMR (126 MHz, DMSO-d_6) δ 165.62, 153.95, 150.86, 146.93, 140.87, 136.70, 133.73, 133.36, 132.57, 129.07, 128.37, 121.63, 121.59, 119.86, 116.69; (ESI-MS) *m/z* = 349.12 $[M+H]^+$, 351.12 $[M+2+H]^+$. HRMS (ESI+) *m/z* calcd. for $C_{19}H_{14}ClN_4O^+$ $[M+H]^+$: 349.0851 found 349.0849.

[3-Amino-5-(pyridin-4-yl)-1*H*-indazol-1-yl]-(2-bromophenyl) methanone (**8**): The title compound was prepared following procedure D using 2-bromobenzoic acid to give a yellow solid: yield (17%). The product was purified by CC (DCM/MeOH 95:5); mp 233–234°C; ^{1}H NMR (500 MHz, DMSO-d_6) δ 8.71 (d, *J* = 6.0 Hz, 2H), 8.47–8.42 (m, 2H), 8.11 (d, *J* = 9.4 Hz, 1H), 7.77 (d, *J* = 6.0 Hz, 2H), 7.72 (d, *J* = 8.0 Hz, 1H), 7.60 (dd, *J* = 7.5, 1.4 Hz, 1H), 7.52 (t, *J* = 7.4 Hz, 1H), 7.44 (t, *J* = 7.7 Hz, 1H), 6.70 (s, 2H); ^{13}C NMR (126 MHz, DMSO-d_6) δ 166.08, 154.16, 150.87, 146.97, 139.95, 138.51, 134.03, 132.65, 131.53, 129.24, 127.92, 123.18, 122.16, 121.71, 120.01, 119.39, 116.25; (ESI-MS) *m/z* = 393.25 $[M+H]^+$, 395.25 $[M+2+H]^+$. HRMS (ESI+) *m/z* calcd. for $C_{19}H_{14}BrN_4O^+$ $[M+H]^+$: 393.0346 found 393.0344.

[3-Amino-5-(pyridin-4-yl)-1*H*-indazol-1-yl]-(3-bromophenyl) methanone (**9**): The title compound was prepared following procedure D using 3-bromobenzoic acid to give a yellow solid: yield (33%). The product was purified by CC (DCM/MeOH 95:5); mp 250–251°C; ^{1}H NMR (500 MHz, DMSO-d_6) δ 8.70 (d, *J* = 6.0 Hz, 2H), 8.47 (dd, *J* = 14.4, 5.0 Hz, 2H), 8.14 (t, *J* = 1.6 Hz, 1H), 8.10 (dd, *J* = 8.6, 1.7 Hz, 1H), 7.96 (d, *J* = 7.8 Hz, 1H), 7.83–7.79 (m, 1H), 7.79–7.77 (m, 2H), 7.51 (t, *J* = 7.9 Hz, 1H), 6.72 (s, 2H); ^{13}C NMR (126 MHz, DMSO-d_6) δ 165.16, 154.06, 150.87, 146.92, 140.80, 136.92, 134.43, 133.84, 132.91, 130.56, 129.44, 129.12, 121.71, 121.64, 121.32, 119.88, 116.70; (ESI-MS) *m/z* = 393.25 $[M+H]^+$, 395.25 $[M+2+H]^+$. HRMS (ESI+) *m/z* calcd. for $C_{19}H_{14}BrN_4O^+$ $[M+H]^+$: 393.0346 found 393.0344.

[3-Amino-5-(pyridin-4-yl)-1*H*-indazol-1-yl]-(4-bromophenyl) methanone (**10**): The title compound was prepared following procedure D using 4-bromobenzoic acid to give a white solid: yield (34%). The product was purified by CC (DCM/MeOH 95:5); mp 240–241°C; ^{1}H NMR (500 MHz, DMSO-d_6) δ 8.70 (d, *J* = 6.0 Hz, 2H), 8.47 (dd, *J* = 10.1, 4.9 Hz, 2H), 8.10 (dd, *J* = 8.6, 1.6 Hz, 1H), 7.95 (d, *J* = 8.5 Hz, 2H), 7.80–7.71 (m, 4H), 6.67 (s, 2H); ^{13}C NMR (126 MHz, DMSO-d_6) δ 165.78, 153.96, 150.85, 146.94, 140.85, 133.75, 132.67, 131.31, 129.08, 125.64, 121.63, 121.60, 119.86, 116.69; (ESI-MS) *m/z* = 393.25 $[M+H]^+$, 395.25 $[M+2+H]^+$. HRMS (ESI+) *m/z* calcd. for $C_{19}H_{14}BrN_4O^+$ $[M+H]^+$: 393.0346 found 393.0344.

[3-Amino-5-(pyridin-4-yl)-1*H*-indazol-1-yl]-[3-(trifluoromethyl) phenyl]methanone (**11**): The title compound was prepared following procedure D using 3-(trifluoromethyl)benzoic acid to give a yellow solid: yield (21%). The product was purified by CC (DCM/MeOH 95:5); mp 205–206°C; ^{1}H NMR (500 MHz, DMSO-d_6) δ 8.69 (d, *J* = 14.4 Hz, 2H), 8.50–8.46 (m, 2H), 8.31–8.22 (m, 3H), 8.18 (s, 1H), 8.11 (dd, *J* = 8.6, 1.5 Hz, 1H), 7.99 (dd, *J* = 19.1, 7.7 Hz, 2H), 6.72 (s, 2H); ^{13}C NMR (126 MHz, DMSO-d_6) δ 165.27, 154.14, 150.88, 146.91, 140.80, 135.78, 134.49, 133.90, 130.56, 129.37 (d, $^{2}J_{C-F}$ = 32.2 Hz), 128.24 (d, $^{3}J_{C-F}$ = 3.6 Hz), 126.96 (d, $^{3}J_{C-F}$ = 3.7 Hz), 124.36 (q, $^{1}J_{C-F}$ = 272.5 Hz), 121.76, 121.64, 119.91, 119.63, 116.70; (ESI-MS) *m/z* = 383.38 $[M+H]^+$. HRMS (ESI+) *m/z* calcd. for $C_{20}H_{14}F_3N_4O^+$ $[M+H]^+$: 383.1114 found 383.1112.

[3-Amino-5-(pyridin-4-yl)-1*H*-indazol-1-yl]-[4-(trifluoromethyl) phenyl]methanone (**12**): The title compound was prepared following procedure D using 4-(trifluoromethyl)benzoic acid to give a yellow solid: yield (19%). The product was purified by CC (DCM/MeOH 95:5); mp 199–200°C; ^{1}H NMR (500 MHz, DMSO-d_6) δ 8.71 (dd, *J* = 4.6, 1.5 Hz, 2H), 8.50–8.46 (m, 2H), 8.15–8.11 (m, 3H), 7.91 (d, *J* = 8.3 Hz, 2H), 7.78 (dd, *J* = 4.6, 1.5 Hz, 2H), 6.71 (s, 2H); ^{13}C NMR (126 MHz, DMSO-d_6) δ 163.60, 152.00, 148.76, 144.78, 138.56, 136.68, 131.84, 129.20 (d, $^{2}J_{C-F}$ = 32.0 Hz), 128.90, 127.08, 123.10 (d, $^{3}J_{C-F}$ = 3.7 Hz), 119.68, 119.53, 117.81, 116.44, 114.53; (ESI-MS) *m/z* = 383.38 $[M+H]^+$. HRMS (ESI+) *m/z* calcd. for $C_{20}H_{14}F_3N_4O^+$ $[M+H]^+$: 383.1114 found 383.1113.

[3-Amino-5-(pyridin-4-yl)-1*H*-indazol-1-yl]-(2-nitrophenyl) methanone (**13**): The title compound was prepared following procedure D using 2-nitrobenzoic acid to give a yellow solid: yield (16%). The product was purified by CC (DCM/MeOH 95:5); mp 180–181°C; ^{1}H NMR (500 MHz, acetone-d_6) δ 8.55 (dd, J = 4.6, 1.5 Hz, 2H), 8.43 (d, J = 8.6 Hz, 1H), 8.23 (d, J = 1.5 Hz, 1H), 8.13 (d, J = 8.2 Hz, 1H), 7.97 (dd, J = 8.6, 1.6 Hz, 1H), 7.83 (t, J = 7.5 Hz, 1H), 7.74–7.68 (m, 2H), 7.63–7.60 (m, 2H), 5.87 (s, 2H); ^{13}C NMR (126 MHz, acetone-d_6) δ 164.58, 153.48, 150.39, 147.18, 146.94, 140.16, 134.44, 134.21, 131.96, 131.23, 130.82, 129.73, 128.81, 123.69, 121.40, 119.11, 115.94; (ESI-MS) m/z = 360.16 $[M+H]^+$. HRMS (ESI+) m/z calcd. for $C_{19}H_{14}N_5O_3^+$ $[M+H]^+$: 360.1091 found 360.1090.

[3-Amino-5-(pyridin-4-yl)-1*H*-indazol-1-yl]-(3-nitrophenyl) methanone (**14**): The title compound was prepared following procedure D using 3-nitrobenzoic acid to give a white solid: yield (22%). The product was purified by CC (DCM/MeOH 95:5); mp 180–181°C; ^{1}H NMR (500 MHz, DMSO-d_6) δ 8.80 (s, 1H), 8.71 (d, J = 5.9 Hz, 2H), 8.52–8.41 (m, 4H), 8.13 (dd, J = 8.6, 1.4 Hz, 1H), 7.85 (t, J = 8.0 Hz, 1H), 7.78 (d, J = 6.0 Hz, 2H), 6.76 (s, 2H); ^{13}C NMR (126 MHz, DMSO-d_6) δ 164.41, 154.26, 150.89, 147.60, 146.87, 140.77, 136.90, 136.14, 134.04, 130.10, 129.26, 126.32, 125.33, 121.83, 121.65, 119.95, 116.75; (ESI-MS) m/z = 360.16 $[M+H]^+$. HRMS (ESI+) m/z calcd. for $C_{19}H_{14}N_5O_3^+$ $[M+H]^+$: 360.1091 found 360.1091.

2-[3-Amino-5-(pyridin-4-yl)-1*H*-indazole-1-carbonyl]benzonitrile (**15**): The title compound was prepared following procedure D using 2-cyanobenzoic acid to give a yellow solid: yield (32%). The product was purified by CC (DCM/MeOH 95:5); mp 186–187°C; ^{1}H NMR (500 MHz, DMSO-d_6) δ 8.59 (d, J = 5 Hz, 2H), 8.41 (dd, J = 16.1, 7.8 Hz, 3H), 8.26 (d, J = 7.7 Hz, 1H), 8.12 (d, J = 8.8 Hz, 1H), 8.07 (d, J = 6.9 Hz, 1H), 7.77 (m, 3H), 6.67 (s, 2H); ^{13}C NMR (126 MHz, DMSO-d_6) δ 165, 154.34, 150.81, 147.37, 139.91, 138.36, 134.43, 132.67, 131.55, 128.89, 127.5, 123.18, 122.24, 121.75, 120.17, 118.92, 116.49, 112.97; (ESI-MS) m/z = 340.34 $[M+H]^+$. HRMS (ESI+) m/z calcd. for $C_{20}H_{14}N_5O^+$ $[M+H]^+$: 340.1193 found 340.1191.

3-[3-Amino-5-(pyridin-4-yl)-1*H*-indazole-1-carbonyl]benzonitrile (**16**): The title compound was prepared following procedure D using 3-cyanobenzoic acid to give a white solid: yield (38%). The product was purified by CC (DCM/MeOH 95:5); mp 191–192°C; ^{1}H NMR (500 MHz, DMSO-d_6) δ 8.70 (d, J = 4.7 Hz, 2H), 8.46 (dd, J = 17.2, 8.2 Hz, 3H), 8.26 (d, J = 7.7 Hz, 1H), 8.15 (d, J = 8.4 Hz, 1H), 8.07 (d, J = 7.2 Hz, 1H), 7.77 (dd, J = 13.2, 6.0 Hz, 3H), 6.75 (s, 2H); ^{13}C NMR (126 MHz, DMSO-d_6) δ 164.77, 154.19, 150.87, 146.89, 140.72, 135.87, 135.15, 134.98, 134.18, 133.99, 129.75, 129.23, 121.79, 121.66, 119.92, 118.85, 116.70, 111.40; (ESI-MS) m/z = 340.34 $[M+H]^+$. HRMS (ESI+) m/z calcd. for $C_{20}H_{14}N_5O^+$ $[M+H]^+$: 340.1193 found 340.1192.

4-[3-Amino-5-(pyridin-4-yl)-1*H*-indazole-1-carbonyl]benzonitrile (**17**): The title compound was prepared following procedure D using 4-cyanobenzoic acid to give a white solid: yield (40%). The product was purified by CC (DCM/MeOH 95:5); mp 188–189°C; ^{1}H NMR (500 MHz, DMSO-d_6) δ 8.76 (d, J = 6.0 Hz, 2H), 8.53 (dd, J = 10.2, 4.8 Hz, 2H), 8.19–8.14 (m, 3H), 8.07 (d, J = 8.3 Hz, 2H), 7.83 (d, J = 6.1 Hz, 2H), 6.79 (s, 2H); ^{13}C NMR (126 MHz, DMSO-d_6) δ 165.40, 154.19, 150.87, 146.89, 140.65, 139.09, 134.04, 132.29, 130.96, 129.23, 121.83, 121.66, 119.93, 118.84, 116.66, 113.85; (ESI-MS) m/z = 340.34 $[M+H]^+$. HRMS (ESI+) m/z calcd. for $C_{20}H_{14}N_5O^+$ $[M+H]^+$: 340.1193 found 340.1193.

1-{2-[3-Amino-5-(pyridin-4-yl)-1*H*-indazole-1-carbonyl]phenyl} ethan-1-one (**18**): The title compound was prepared following procedure D using 2-acetylbenzoic acid to give a yellow solid: yield (20%). The product was purified by CC (DCM/MeOH 95:5); mp 218–219°C; ^{1}H NMR (500 MHz, DMSO-d_6) δ 8.67 (d, J = 6.1 Hz, 2H), 8.40 (dd, J = 16.1, 4.9 Hz, 2H), 8.08–8.04 (m, 1H), 7.99 (d, J = 7.4 Hz, 1H), 7.75–7.73 (m, 1H), 7.68 (d, J = 7.2 Hz, 2H), 7.62 (dd, J = 10.4, 7.4 Hz, 2H), 6.49 (s, 2H), 2.53 (s, 3H); ^{13}C NMR (126 MHz, DMSO-d_6) δ 199.34, 168.12, 153.37, 150.76, 147.13, 140.25, 138.19, 135.45, 133.34, 132.25, 130.23, 129.00, 124.91, 121.64, 121.40, 121.09, 119.85, 116.09, 27.80; (ESI-MS) m/z = 357.34 $[M+H]^+$. HRMS (ESI+) m/z calcd. for $C_{21}H_{17}N_4O_2^+$ $[M+H]^+$: 357.1346 found 357.1344.

1-{4-[3-Amino-5-(pyridin-4-yl)-1*H*-indazole-1-carbonyl]phenyl} ethan-1-one (**19**): The title compound was prepared following procedure D using 4-acetylbenzoic acid to give a yellow solid: yield (36%). The product was purified by CC (DCM/MeOH 95:5); mp 232–233°C; ^{1}H NMR (500 MHz, DMSO-d_6) δ 8.71 (d, J = 6.0 Hz, 2H), 8.48 (dd, J = 8.6, 4.9 Hz, 2H), 8.12 (dd, J = 8.6, 1.7 Hz, 1H), 8.07 (q, J = 8.4 Hz, 4H), 7.78 (dd, J = 4.7, 1.4 Hz, 2H), 6.69 (s, 2H), 2.67 (s, 3H); ^{13}C NMR (126 MHz, DMSO-d_6) δ 198.23, 166.22, 154.04, 150.88, 146.92, 140.74, 138.83, 133.87, 130.52,130.11, 129.14, 127.98, 121.74, 121.65, 119.91, 116.65, 27.50; (ESI-MS) m/z = 357.34 $[M+H]^+$. HRMS (ESI+) m/z calcd. for $C_{21}H_{17}N_4O_2^+$ $[M+H]^+$: 357.1346 found 357.1343.

[3-Amino-5-(pyridin-4-yl)-1*H*-indazol-1-yl]-(*o*-tolyl)methanone (**20**): The title compound was prepared following procedure D using 2-methylbenzoic acid to give a yellow solid: yield (32%). The product was purified by CC (DCM/MeOH 95:5); mp 165–166°C; ^{1}H NMR (500 MHz, DMSO-d_6) δ 8.66 (d, J = 5.9 Hz, 2H), 8.42 (d, J = 15.5 Hz, 2H), 8.08 (d, J = 8.7 Hz, 1H), 7.77 (d, J = 6.1 Hz, 2H), 7.39 (dd, J = 11.0, 7.5 Hz, 2H), 7.28 (dd, J = 20.3, 12.3 Hz, 2H), 6.55 (s, 2H), 2.22 (s, 3H); ^{13}C NMR (126 MHz, DMSO-d_6) δ 168.54, 153.98, 150.65, 147.16, 141.39, 140.17, 136.42, 135.09, 133.79, 130.37, 129.99, 129.07, 127.78, 125.75, 121.74, 119.76, 116.36, 19.39; (ESI-MS) m/z = 329.34 $[M+H]^+$. HRMS (ESI+) m/z calcd. for $C_{20}H_{17}N_4O^+$ $[M+H]^+$: 329.1397 found 329.1394.

[3-Amino-5-(pyridin-4-yl)-1*H*-indazol-1-yl]-(*m*-tolyl)methanone (**21**): The title compound was prepared following procedure D using 3-methylbenzoic acid to give a yellow solid: yield (40%). The product was purified by CC (DCM/MeOH 95:5); mp 171–172°C; ^{1}H NMR (500 MHz, DMSO-d_6) δ 8.70 (d, J = 4.6 Hz, 2H), 8.46 (dd, J = 9.2, 3.5 Hz, 2H), 8.12–8.06 (m, 1H), 7.77 (d, J = 6.8 Hz, 4H), 7.41 (s, 2H), 6.62 (s, 2H), 2.41 (s, 3H); ^{13}C NMR (126 MHz, DMSO-d_6) δ 167.08, 153.76, 150.85, 146.99, 140.91, 137.49, 134.74, 133.52, 132.34, 130.73, 128.94, 128.13, 127.72, 121.63, 121.49, 119.79, 116.65, 21.44; (ESI-MS) m/z = 329.34 $[M+H]^+$. HRMS (ESI+) m/z calcd. for $C_{20}H_{17}N_4O^+$ $[M+H]^+$: 329.1397 found 329.1393.

[3-Amino-5-(pyridin-4-yl)-1*H*-indazol-1-yl]-(*p*-tolyl)methanone (**22**): The title compound was prepared following procedure D using 4-methylbenzoic acid to give a white solid: yield (28%). The product was purified by CC (DCM/MeOH 95:5); mp 155–156°C; ^{1}H NMR (500 MHz, DMSO-d_6) δ 8.70 (d, J = 6.0 Hz, 2H), 8.48–8.43 (m, 2H), 8.08 (dd, J = 8.7, 1.6 Hz, 1H), 7.93 (d, J = 8.1 Hz, 2H), 7.77 (d, J = 6.0 Hz, 2H), 7.34 (d, J = 8.0 Hz, 2H), 6.61 (s, 2H), 2.41 (s, 3H); ^{13}C NMR (126 MHz, DMSO-d_6) δ 166.70, 153.69, 150.85, 147.00, 142.01, 141.01, 133.42, 131.68, 130.86, 128.89, 128.79, 121.61, 121.37, 119.78, 116.68, 21.59; (ESI-MS) m/z = 329.34 $[M+H]^+$. HRMS (ESI+) m/z calcd. for $C_{20}H_{17}N_4O^+$ $[M+H]^+$: 329.1397 found 329.1395.

[3-Amino-5-(pyridin-4-yl)-1H-indazol-1-yl]-(2-methoxyphenyl) methanone (**23**): The title compound was prepared following procedure D using 2-methoxybenzoic acid to give a white solid: yield (23%). The product was purified by CC (DCM/MeOH 95:5); mp 211–212°C; ^{1}H NMR (500 MHz, DMSO-d_6) δ 8.70 (d, J = 5.8 Hz, 2H), 8.44 (s, 2H), 8.08 (d, J = 8.2 Hz, 1H), 7.77 (d, J = 5.4 Hz, 2H), 7.47 (t, J = 7.8 Hz, 1H), 7.39 (d, J = 7.0 Hz, 1H), 7.15 (d, J = 8.4 Hz, 1H), 7.05 (t, J = 7.4 Hz, 1H), 6.54 (s, 2H), 3.76 (s, 3H); ^{13}C NMR (126 MHz, DMSO-d_6) δ 156.41, 153.58, 150.78, 147.07, 140.07, 133.55, 133.51, 131.30, 128.79, 128.46, 126.52, 121.86, 121.58, 120.45, 119.78, 116.10, 112.10, 55.98; (ESI-MS) m/z = 345.34 $[M+H]^+$. HRMS (ESI+) m/z calcd. for $C_{20}H_{17}N_4O_2^+$ $[M+H]^+$: 345.1346 found 345.1345.

[3-Amino-5-(pyridin-4-yl)-1*H*-indazol-1-yl]-(3-methoxyphenyl) methanone (**24**): The title compound was prepared following procedure D using 3-methoxybenzoic acid to give a white solid: yield (30%). The product was purified by CC (DCM/MeOH 95:5); mp 196–197°C; ^{1}H NMR (500 MHz, DMSO-d_6) δ 8.70 (d, J = 5.8 Hz, 2H), 8.49–8.44 (m, 2H), 8.09 (dd, J = 8.6, 1.5 Hz, 1H), 7.77 (d, J = 5.9 Hz, 2H), 7.54 (dd, J = 10.1, 4.9 Hz, 2H), 7.45 (t, J = 7.9 Hz, 1H), 7.17 (dd, J = 8.2, 2.4 Hz, 1H), 6.65 (s, 2H), 3.83 (s, 3H); ^{13}C NMR (126 MHz, DMSO-d_6) δ 166.56, 158.97, 153.81, 150.86, 146.97, 140.93, 135.92, 133.59, 129.42, 128.97, 122.76, 121.62, 121.55, 119.81, 117.27, 116.66, 116.05, 55.78; (ESI-MS) m/z = 345.34 $[M+H]^+$. HRMS (ESI+) m/z calcd. for $C_{20}H_{17}N_4O_2^+$ $[M+H]^+$: 345.1346 found 345.1344.

[3-Amino-5-(pyridin-4-yl)-1*H*-indazol-1-yl]-(4-methoxyphenyl) methanone (**25**): The title compound was prepared following procedure D using 4-methoxybenzoic acid to give a white solid: yield (24%). The product was purified by CC (DCM/MeOH 95:5); mp 205–206°C; ^{1}H NMR (500 MHz, DMSO-d_6) δ 8.71–8.69 (m, 2H), 8.49–8.44 (m, 2H), 8.11 (t, J = 5.8 Hz, 2H), 8.07 (dd, J = 8.7, 1.7 Hz, 1H), 7.77 (dd, J = 4.7, 1.5 Hz, 2H), 7.08 (t, J = 5.8 Hz, 2H), 6.60 (s, 2H), 3.87 (s, 3H); ^{13}C NMR (126 MHz, DMSO-d_6) δ 165.94, 162.40, 153.61, 150.85, 147.03, 141.18, 133.33, 133.27, 128.84, 126.31, 121.60, 121.18, 119.74, 116.72, 113.61, 55.94; (ESI-MS) m/z = 345.34 $[M+H]^+$. HRMS (ESI+) m/z calcd. for $C_{20}H_{17}N_4O_2^+$ $[M+H]^+$: 345.1346 found 345.1344.

[3-Amino-5-(pyridin-4-yl)-1*H*-indazol-1-yl]-[3-(hydroxymethyl) phenyl]methanone (**26**): The title compound was prepared following procedure D using 3-(hydroxymethyl)benzoic acid to give a white solid: yield (17%). The product was purified by CC (DCM/MeOH 95:5); mp 188–189°C; ^{1}H NMR (500 MHz, DMSO-d_6) δ 8.70 (d, J = 6.0 Hz, 2H), 8.46 (d, J = 8.8 Hz, 2H), 8.09 (dd, J = 8.6, 1.6 Hz, 1H), 7.89–7.85 (m, 2H), 7.78 (d, J = 6.1 Hz, 2H), 7.50 (dt, J = 15.1, 7.6 Hz, 2H), 6.62 (s, 2H), 5.35 (s, 1H), 4.59 (d, J = 5.4 Hz, 2H); ^{13}C NMR (126 MHz, DMSO-d_6) δ 167.12, 153.78, 150.85, 147.00, 142.69, 140.92, 134.57, 133.55, 129.74, 128.98, 128.96, 128.18, 127.97, 121.63, 121.50, 119.80, 116.67, 63.03; (ESI-MS) m/z = 345.34 $[M+H]^+$. HRMS (ESI+) m/z calcd. for $C_{20}H_{17}N_4O_2^+$ $[M+H]^+$: 345.1346 found 345.1344.

[3-Amino-5-(pyridin-4-yl)-1*H*-indazol-1-yl]-(3,5-difluorophenyl) methanone (**27**): The title compound was prepared following procedure D using 3,5-difluorobenzoic acid to give a white solid: yield (36%). The product was purified by CC (DCM/MeOH 95:5); mp 200–201°C; ^{1}H NMR (500 MHz, DMSO-d_6) δ 8.70 (d, J = 5.6 Hz, 2H), 8.47 (d, J = 9.0 Hz, 1H), 8.45 (d, J = 8.6 Hz, 1H), 8.11 (dd, J = 8.6, 1.3 Hz, 1H), 7.77 (d, J = 5.9 Hz, 2H), 7.72 (d, J = 5.9 Hz, 2H), 7.56–7.50 (m, 1H), 6.77 (s, 2H); ^{13}C NMR (126 MHz, DMSO-d_6) δ 163.93, 162.07 (d, $^1J_{C-F}$ = 246.5 Hz), 161.97 (d, $^1J_{C-F}$ = 246.7 Hz), 154.21, 150.87, 146.87, 140.77, 137.87 (t, $^3J_{C-F}$ = 9.4 Hz), 134.03, 129.24, 121.83, 121.65, 119.93, 116.71, 113.93 (d, $^3J_{C-F}$ = 14.3 Hz), 113.93 (d, $^2J_{C-F}$ = 27.5 Hz), 107.21 (t, $^2J_{C-F}$ = 25.7 Hz); (ESI-MS) m/z = 351.34 $[M+H]^+$. HRMS (ESI+) m/z calcd. for $C_{19}H_{13}F_2N_4O^+$ $[M+H]^+$: 351.1052 found 351.1048.

[3-Amino-5-(pyridin-4-yl)-1*H*-indazol-1-yl]-(3,4,5-trifluorophenyl) methanone (**28**): The title compound was prepared following procedure D using 3,4,5-trifluorobenzoic acid to give a white solid: yield (38%). The product was purified by CC (DCM/MeOH 95:5); mp 169–170°C; ^{1}H NMR (500 MHz, DMSO-d_6) δ 8.70 (d, J = 3.5 Hz, 2H), 8.48 (d, J = 11.3 Hz, 1H), 8.44 (d, J = 8.3 Hz, 1H), 8.11 (d, J = 8.4 Hz, 1H), 8.06–8.00 (m, 2H), 7.77 (d, J = 3.6 Hz, 2H), 6.79 (s, 2H); ^{13}C NMR (126 MHz, DMSO-d_6) δ 162.95, 154.27, 150.87, 149.02 (d, $^4J_{C-F}$ = 3.2 Hz), 148.95, 146.84, 140.83, 134.07, 130.11, 129.30, 121.78, 121.65, 119.95, 116.75, 116.05 (d, $^2J_{C-F}$ = 23.0 Hz), 116.05 (d, $^3J_{C-F}$ = 12.9 Hz); (ESI-MS) m/z = 369.34 $[M+H]^+$. HRMS (ESI+) m/z calcd. for $C_{19}H_{12}F_3N_4O^+$ $[M+H]^+$: 369.0958 found 369.0958.

[3-Amino-5-(pyridin-4-yl)-1*H*-indazol-1-yl]-(2,4-dichlorophenyl) methanone (**29**): The title compound was prepared following procedure D using 2,4-dichlorobenzoic acid to give a white solid: yield (37%). The product was purified by CC (DCM/MeOH 95:5); mp 164–165°C; ^{1}H NMR (500 MHz, DMSO-d_6) δ 8.70 (d, J = 5.8 Hz, 2H), 8.44 (d, J = 10.7 Hz, 2H), 8.11 (d, J = 8.5 Hz, 1H), 7.77 (dd, J = 9.5, 3.7 Hz, 3H), 7.70 (d, J = 8.2 Hz, 1H), 7.58 (dd, J = 8.2, 1.6 Hz, 1H), 6.73 (s, 2H); ^{13}C NMR (126 MHz, DMSO-d_6) δ 164.36, 154.30, 150.87, 146.91, 139.85, 135.32, 135.24, 134.27, 131.55, 130.71, 129.33, 129.30, 127.80, 122.23, 121.70, 120.06, 116.22; (ESI-MS) m/z = 383.12 $[M+H]^+$, 385.13 $[M+2+H]^+$. HRMS (ESI+) m/z calcd. for $C_{19}H_{13}Cl_2N_4O^+$ $[M+H]^+$: 383.0461 found 383.0460.

[3-Amino-5-(pyridin-4-yl)-1*H*-indazol-1-yl]-(2-hydroxy-4-methoxyphenyl)methanone (**30**): The title compound was prepared following procedure D using 2-hydroxy-4-methoxybenzoic acid to give a white solid: yield (34%). The product was purified by CC (DCM/MeOH 94:6); mp 167–168°C; ^{1}H NMR (500 MHz, DMSO-d_6) δ 9.51 (s, 1H), 8.67 (d, J = 5.9 Hz, 2H), 8.44 (s, 1H), 8.38 (d, J = 8.7 Hz, 1H), 8.05 (dd, J = 8.7, 1.5 Hz, 1H), 7.83 (d, J = 8.7 Hz, 1H), 7.74 (d, J = 6.0 Hz, 2H), 6.65 (s, 2H), 6.50 (dd, J = 8.7, 2.4 Hz, 1H), 6.46 (d, J = 2.3 Hz, 1H), 3.78 (s, 3H); ^{13}C NMR (126 MHz, DMSO-d_6) δ

166.99, 163.19, 159.46, 153.74, 150.81, 146.93, 140.74, 133.36, 132.66, 128.92, 121.56, 121.33, 119.78, 116.63, 114.11, 105.77, 101.83, 55.77; (ESI-MS) m/z = 361.41 $[M+H]^+$. HRMS (ESI+) m/z calcd. for $C_{20}H_{17}N_4O_3^+$ $[M+H]^+$: 361.1295 found 361.1294.

4.1.6 | Procedure E, general procedure for the dealkylation reaction to give **23a** and **24a**

The corresponding methoxy derivative (**23** or **24**) (0.3 mmol, 1 equiv) was dissolved in 50 mL dichloromethane and allowed to stir on ice for 10 min then 1 M borontribromide (1.5 mmol, 5 equiv) were added dropwise via syringe to the reaction flask and left at room temperature overnight. A mixture of methanol and distilled water (3:1) was added to quench the reaction till no fumes appeared, and the solvents were concentrated under reduced pressure until dried. The product was precipitated as pure crystals collected by filtration.

[3-Amino-5-(pyridin-4-yl)-1*H*-indazol-1-yl]-(2-hydroxyphenyl) methanone (**23a**): The title compound was prepared following procedure E using compound **23** to give a white solid: yield (18%). The product was purified by CC (DCM/MeOH 94:6); mp 240–241°C; ^{1}H NMR (500 MHz, DMSO-d_6) δ 9.96 (s, 1H), 8.91 (d, J = 6.0 Hz, 2H), 8.63 (s, 1H), 8.44 (d, J = 7.6 Hz, 1H), 8.23–8.17 (m, 3H), 7.41 (dd, J = 7.5, 1.4 Hz, 1H), 7.32 (t, J = 7.1 Hz, 1H), 6.95–6.87 (m, 2H), 6.71 (s, J = 67.7 Hz, 2H); ^{13}C NMR (126 MHz, DMSO-d_6) δ 167.40, 155.11, 153.60, 152.50, 145.84, 140.93, 131.62, 131.34, 129.41, 129.25, 124.04, 123.07, 121.82, 121.17, 118.93, 116.52, 116.41; (ESI-MS) m/z = 331.21 $[M+H]^+$. HRMS (ESI+) m/z calcd. for $C_{19}H_{15}N_4O_2^+$ $[M+H]^+$: 331.1190 found 331.1186.

[3-Amino-5-(pyridin-4-yl)-1*H*-indazol-1-yl]-(3-hydroxyphenyl) methanone (**24a**): The title compound was prepared following procedure E using compound **24** to give a yellow solid: yield (27%). The product was purified by CC (DCM/MeOH 94:6); mp 217–218°C; ^{1}H NMR (500 MHz, DMSO-d_6) δ 8.91 (d, J = 6.6 Hz, 2H), 8.67 (d, J = 1.0 Hz, 1H), 8.48 (t, J = 7.6 Hz, 1H), 8.36 (d, J = 6.7 Hz, 2H), 8.24 (dd, J = 8.8, 1.6 Hz, 1H), 7.41–7.26 (m, 3H), 6.99 (dd, J = 8.0, 1.6 Hz, 1H); ^{13}C NMR (126 MHz, DMSO-d_6) δ 167.16, 157.03, 154.98, 153.68, 143.36, 141.96, 135.42, 130.63, 129.72, 129.47, 123.85, 121.61, 121.49, 121.35, 119.03, 117.21, 116.97; (ESI-MS) m/z = 331.21 $[M+H]^+$. HRMS (ESI+) m/z calcd. for $C_{19}H_{15}N_4O_2^+$ $[M+H]^+$: 331.1190 found 331.11854.2.31.

4.2 | Biological assays

4.2.1 | PKs and inhibition assays

Haspin kinase assay

The kinase assay was done at (Thermo Fisher Scientific) through a fluorescence-based immunoassay known as the "Adapta Universal Kinase Assay", which detects the ADP produced by kinases utilizing the TR-FRET technology. The final 10 µL kinase reaction consists of 0.25–1 ng GSG2 (haspin) and 100 µM of the substrate (histone H3 (1–20) peptide) in 32.5 mM HEPES pH 7.5, 0.005% BRIJ-35, 5 mM $MgCl_2$, 0.5 mM EGTA, in the presence of 25 µM ATP. After an incubation time of 1 h at RT, 5 µL of a detection mix was added. Staurosporine (IC_{50} = 7.7 nM) was used as a positive control. To determine the half maximal inhibitory concentration (IC_{50}), the assays were performed in duplicate in the absence or presence of increasing doses of the tested compounds.

Clk4 kinase assay

The Kinase assay was done at (Thermo Fisher Scientific) through a LanthaScreen Eu Kinase Binding Assay which employs the Binding of an Alexa Fluor™ conjugate or "tracer" to a kinase detected by addition of a Eu-labeled anti-tag antibody. Binding of the tracer and antibody to a kinase results in a high degree of FRET, whereas displacement of the tracer with a kinase inhibitor results in a loss of FRET. Unlike many kinase activity assays, this assay is a simple mix-and-read assay, with no development steps. The test was performed in a bar-coded, low volume, white 384-well plate that constitue of: 160 nL—100X test compound in 100% DMSO, 3.84 µL—Kinase Buffer (50 mM HEPES pH 7.5, 0.01% BRIJ-35, 10 mM $MgCl_2$, 1 mM EGTA), 8.0 µL—2X Kinase/Antibody mixture, 4.0 µL—4X Tracer then subjected to 30-s plate shake and 60-min incubation at RT. Finally, it was put on a fluorescence plate reader and analyze the data. Staurosporine (IC_{50} = 7.02 nM) was used as a positive control. To determine the half maximal IC_{50}, the assays were performed in duplicate in the absence or presence of increasing doses of the tested compounds.

SelectScreen kinase profiling (Thermo Fisher Scientific)

This screen utilized three different assays appropriate to each kinase, its substrate, and its activity: a binding assay (LanthaScreen TR-FRET technology) and two activity assays (Z0-LYTE or Adapta). The LanthaScreen Eu Kinase Binding Assay utilizes an Alexa Fluor conjugated "tracer" and a Eu-labeled anti-tag antibody to measure binding of a compound to the kinase target. The Z0-LYTE Kinase Assay determines the differential sensitivity of phosphorylated and nonphosphorylated peptide substrates using a FRET-based readout. The Adapta Universal Kinase Assay is a fluorescence-based immunoassay for the detection of ADP produced by kinases utilizing the TR-FRET technology. For the activity assays, the used ATP concentrations were set at the approximative K_m for each kinase. For more information, see the SelectScreen Kinase Profiling Services on ThermoFisher website.

4.2.2 | Anticancer NCI cell-based screening

Compounds **X**, **5**, **13**, **17**, **18**, **19**, **23a**, and **24a** were submitted for anticancer activity screening against 60 different cell lines, representing nine different human tissues, by the Developmental Therapeutics Program of the United States National Cancer Institute, Bethesda, MD.[38] The NCI-60 screen was done by

employing the SRB assay. The results provided are growth percentages relative to the no-drug control and relative to the time zero number of cells. Values of percentage growth inhibition (% GI) were calculated from the values of mean growth percentages as (100 − growth %).

4.3 | In silico studies

4.3.1 | In silico physicochemical properties and ADME prediction

Molecular structures of the compounds were converted into SMILES using ChemDraw12.0. The SMILES were used as an input in the web-based Swiss-ADME tool, http://www.Swissadme.ch/index.php, to calculate the physicochemical descriptors to evaluate pharmacokinetics and drug-likeness and medicinal chemistry friendliness. Furthermore, the Swiss-ADME tool was used for prediction of permeability through the human gastrointestinal tract and BBB.

4.3.2 | Molecular docking simulation

Docking studies were carried out essentially as described in Elhady et al.[25] All procedures were performed using the molecular operating environment (MOE) software package (version 2014. Chemical Computing Group). PDB entry: 7OPS for haspin and 6FYV for Clk4 were used for docking simulations. Molecular docking simulations employing compounds **18** and **19** as ligands were conducted using the MMFF94x force field and the "alpha pmi" method with the number of return poses set to 100 and "Forcefield" as refinement. A pharmacophore was defined based on a suitable pose after energy minimization using the MOE LigX routine (settings: receptor strength = 1, ligand strength = 30). Within the pharmacophore definition window, the radius of the pharmacophore points was increased to 1.6 Å. Subsequently, compounds **18** and **19** were docked in the ATP binding pocket of haspin and Clk4, respectively was performed using the pharmacophore–supported placement. The number of retained poses was set to 100 each time. Only the poses with the top 10 scoring values underwent additional evaluation for plausibility. The final selected poses were optimized again using the LigX routine.

ACKNOWLEDGMENTS

The authors would like to thank the National Cancer Institute (USA)—Development Therapeutics Program (DTP) for testing some of the compounds presented in this work. Open Access funding enabled and organized by Projekt DEAL.

CONFLICTS OF INTEREST STATEMENT

The authors declare no conflicts of interest.

DATA AVAILABILITY STATEMENT

The data that support the findings of this study are available from the corresponding author upon reasonable request.

ORCID

Habiba G. Aboelfotouh https://orcid.org/0009-0003-7241-7761
Mennatallah Abdallah http://orcid.org/0009-0008-3797-8033
Hend Khalifa http://orcid.org/0009-0007-0407-7645
Ashraf H. Abadi http://orcid.org/0000-0002-7433-261X
Matthias Engel http://orcid.org/0000-0001-5065-8634
Mohammad Abdel-Halim http://orcid.org/0000-0003-1326-4219

REFERENCES

[1] S. Cheek, H. Zhang, N. V. Grishin, *J. Mol. Biol.* **2002**, *320*, 855. https://doi.org/10.1016/S0022-2836(02)00538-7
[2] S. H. Seok, *Life* **2021**, *11*, 957. https://doi.org/10.3390/life11090957
[3] H. C. Cheng, R. Z. Qi, H. Paudel, H. J. Zhu, *Enzyme Res.* **2011**, *2011*, 1. https://doi.org/10.4061/2011/794089
[4] C. J. Tsai, R. Nussinov, *Semin. Cancer Biol.* **2013**, *23*, 235. https://doi.org/10.1016/j.semcancer.2013.04.001
[5] J. Zhang, P. L. Yang, N. S. Gray, *Nat. Rev. Cancer* **2009**, *9*, 28. https://doi.org/10.1038/nrc2559
[6] R. Roskoski, *Pharmacol. Res.* **2023**, *191*, 106774. https://doi.org/10.1016/j.phrs.2023.106774
[7] J. Eswaran, D. Patnaik, P. Filippakopoulos, F. Wang, R. L. Stein, J. W. Murray, J. M. G. Higgins, S. Knapp, *Proc. Natl. Acad. Sci. U.S.A.* **2009**, *106*, 20198. https://doi.org/10.1073/pnas.0901989106
[8] J. M. G. Higgins, *Protein Sci.* **2001**, *10*, 1677. https://doi.org/10.1110/ps.49901
[9] J. Dai, S. Sultan, S. S. Taylor, J. M. G. Higgins, *Genes Dev.* **2005**, *19*, 472. https://doi.org/10.1101/gad.1267105
[10] R. Quadri, S. Sertic, M. Muzi-Falconi, *Cell. Signal.* **2022**, *93*, 110303. https://doi.org/10.1016/j.cellsig.2022.110303
[11] Y. Huang, Y. Liu, K. Zhu, X. Ma, R. Lu, M. Zhang, *Cancer Manag. Res.* **2021**, *13*, 499. https://doi.org/10.2147/CMAR.S274807
[12] H. Nishida-Fukuda, K. Tokuhiro, Y. Ando, H. Matsushita, M. Wada, H. Tanaka, *PLoS One* **2021**, *16*, e0249912. https://doi.org/10.1371/journal.pone.0249912
[13] C. I. Lin, Z. C. Chen, C. H. Chen, Y. H. Chang, T. C. Lee, T. T. Tang, T. W. Yu, C. M. Yang, M. C. Tsai, C. C. Huang, T. W. Yang, C. C. Lin, R. H. Wang, G. Y. Chiou, Y. J. Jong, J. I. Chao, *Biochem. Pharmacol.* **2022**, *206*, 115289. https://doi.org/10.1016/j.bcp.2022.115289
[14] D. Huertas, M. Soler, J. Moreto, A. Villanueva, A. Martinez, A. Vidal, M. Charlton, D. Moffat, S. Patel, J. McDermott, J. Owen, D. Brotherton, D. Krige, S. Cuthill, M. Esteller, *Oncogene* **2012**, *31*, 1408. https://doi.org/10.1038/onc.2011.335
[15] N. G. Amoussou, A. Bigot, C. Roussakis, J. M. H. Robert, *Drug Discov. Today* **2018**, *23*, 409. https://doi.org/10.1016/j.drudis.2017.10.005
[16] K. Kestav, A. Uri, D. Lavogina, *Curr. Med. Chem.* **2017**, *24*, 2276. https://doi.org/10.2174/0929867324666170414155520
[17] M. Murugan, D. Fedele, D. Millner, E. Alharfoush, G. Vegunta, D. Boison, *Neurochem. Int.* **2021**, *147*, 105054. https://doi.org/10.1016/j.neuint.2021.105054
[18] A. De Antoni, S. Maffini, S. Knapp, A. Musacchio, S. Santaguida, *J. Cell Biol.* **2012**, *199*, 269. https://doi.org/10.1083/jcb.201205119
[19] D. Massillon, W. Stalmans, G. Van de Werve, M. Bollen, *Biochem. J.* **1994**, *299*, 123. https://doi.org/10.1042/bj2990123
[20] W. Zeinyeh, Y. J. Esvan, B. Josselin, M. Defois, B. Baratte, S. Knapp, A. Chaikuad, F. Anizon, F. Giraud, S. Ruchaud, P. Moreau, *Eur.*

J. Med. Chem. **2022**, *236*, 114369. https://doi.org/10.1016/j.ejmech.2022.114369

[21] G. D. Cuny, M. Robin, N. P. Ulyanova, D. Patnaik, V. Pique, G. Casano, J. F. Liu, X. Lin, J. Xian, M. A. Glicksman, R. L. Stein, J. M. G. Higgins, *Bioorg. Med. Chem. Lett.* **2010**, *20*, 3491. https://doi.org/10.1016/j.bmcl.2010.04.150

[22] D. Patnaik, J. Xian, M. A. Glicksman, G. D. Cuny, R. L. Stein, J. M. G. Higgins, *SLAS Discov.* **2008**, *13*, 1025. https://doi.org/10.1177/1087057108326081

[23] J. Elie, O. Feizbakhsh, N. Desban, B. Josselin, B. Baratte, A. Bescond, J. Duez, X. Fant, S. Bach, D. Marie, M. Place, S. Ben Salah, A. Chartier, S. Berteina-Raboin, A. Chaikuad, S. Knapp, F. Carles, P. Bonnet, F. Buron, S. Routier, S. Ruchaud, *J. Enzyme Inhib. Med. Chem.* **2020**, *35*, 1840. https://doi.org/10.1080/14756366.2020.1825408

[24] P. M. Moyano, V. Němec, K. Paruch, *Int. J. Mol. Sci.* **2020**, *21*, 1. https://doi.org/10.3390/ijms21207549

[25] A. K. Elhady, M. Abdel-Halim, A. H. Abadi, M. Engel, *J. Med. Chem.* **2017**, *60*, 5377. https://doi.org/10.1021/acs.jmedchem.6b01915

[26] A. C. Blackie, D. J. Foley, *Bioorg. Med. Chem.* **2022**, *70*, 116914. https://doi.org/10.1016/j.bmc.2022.116914

[27] M. F. Al-Tawil, S. Daoud, M. M. Hatmal, M. O. Taha, *RSC Adv.* **2022**, *12*, 10686. https://doi.org/10.1039/d2ra00136e

[28] M. Capra, P. G. Nuciforo, S. Confalonieri, M. Quarto, M. Bianchi, M. Nebuloni, R. Boldorini, F. Pallotti, G. Viale, M. L. Gishizky, G. F. Draetta, P. P. Di Fiore, *Cancer Res.* **2006**, *66*, 8147. https://doi.org/10.1158/0008-5472.CAN-05-3489

[29] M. Song, L. Pang, M. Zhang, Y. Qu, K. V. Laster, Z. Dong, *Signal Transduct. Target. Ther.* **2023**, *8*, 148. https://doi.org/10.1038/s41392-023-01409-4

[30] A. K. ElHady, D. S. El-Gamil, A. H. Abadi, M. Abdel-Halim, M. Engel, *Med. Res. Rev.* **2023**, *43*, 343. https://doi.org/10.1002/med.21928

[31] D. S. El-Gamil, A. K. ElHady, P. J. Chen, T. L. Hwang, A. H. Abadi, M. Abdel-Halim, M. Engel, *Eur. J. Med. Chem.* **2022**, *238*, 114411. https://doi.org/10.1016/j.ejmech.2022.114411

[32] D. S. El-Gamil, A. K. ElHady, P. J. Chen, T. L. Hwang, A. H. Abadi, M. Abdel-Halim, M. Engel, *Eur. J. Med. Chem.* **2023**, *247*, 115019. https://doi.org/10.1016/j.ejmech.2022.115019

[33] J. Kallen, C. Bergsdorf, B. Arnaud, M. Bernhard, M. Brichet, A. Cobos-Correa, A. Elhajouji, F. Freuler, I. Galimberti, C. Guibourdenche, S. Haenni, S. Holzinger, J. Hunziker, A. Izaac, M. Kaufmann, L. Leder, H. J. Martus, P. von Matt, V. Polyakov, P. Roethlisberger, G. Roma, N. Stiefl, M. Uteng, A. Lerchner, *ChemMedChem* **2018**, *13*, 1997. https://doi.org/10.1002/cmdc.201800344

[34] K. Iwai, M. Yaguchi, K. Nishimura, Y. Yamamoto, T. Tamura, D. Nakata, R. Dairiki, Y. Kawakita, R. Mizojiri, Y. Ito, M. Asano, H. Maezaki, Y. Nakayama, M. Kaishima, K. Hayashi, M. Teratani, S. Miyakawa, M. Iwatani, M. Miyamoto, M. G. Klein, W. Lane, G. Snell, R. Tjhen, X. He, S. Pulukuri, T. Nomura, *EMBO Mol. Med.* **2018**, *10*, 1. https://doi.org/10.15252/emmm.201708289

[35] B. Y. Tam, K. Chiu, H. Chung, C. Bossard, J. D. Nguyen, E. Creger, B. W. Eastman, C. C. Mak, M. Ibanez, A. Ghias, J. Cahiwat, L. Do, S. Cho, J. Nguyen, V. Deshmukh, J. Stewart, C. W. Chen, C. Barroga, L. Dellamary, S. K. KC, T. J. Phalen, J. Hood, S. Cha, Y. Yazici, *Cancer Lett.* **2020**, *473*, 186. https://doi.org/10.1016/j.canlet.2019.09.009

[36] M. Muraki, B. Ohkawara, T. Hosoya, H. Onogi, J. Koizumi, T. Koizumi, K. Sumi, J. Yomoda, M. V. Murray, H. Kimura, K. Furuichi, H. Shibuya, A. R. Krainer, M. Suzuki, M. Hagiwara, *J. Biol. Chem.* **2004**, *279*, 24246. https://doi.org/10.1074/jbc.M314298200

[37] A. S. Rosenthal, C. Tanega, M. Shen, B. T. Mott, J. M. Bougie, D. T. Nguyen, T. Misteli, D. S. Auld, D. J. Maloney, C. J. Thomas, *Bioorg. Med. Chem. Lett.* **2011**, *21*, 3152. https://doi.org/10.1016/j.bmcl.2011.02.114

[38] R. H. Shoemaker, *Nat. Rev. Cancer* **2006**, *6*, 813. https://doi.org/10.1038/nrc1951

[39] A. Daina, O. Michielin, V. Zoete, *Sci. Rep.* **2017**, *7*, 42717. https://doi.org/10.1038/srep42717

[40] R. Brenk, A. Schipani, D. James, A. Krasowski, I. H. Gilbert, J. Frearson, P. G. Wyatt, *ChemMedChem* **2008**, *3*, 435. https://doi.org/10.1002/cmdc.200700139

[41] A. Daina, V. Zoet, *ChemMedChem* **2016**, *11*, 1117. https://doi.org/10.1002/cmdc.201600182

[42] C. E. Adkins, R. K. Mittapalli, V. K. Manda, M. I. Nounou, A. S. Mohammad, T. B. Terrell, K. A. Bohn, C. Yasemin, T. R. Grothe, J. A. Lockman, P. R. Lockman, *Front. Pharmacol.* **2013**, *4*, 1. https://doi.org/10.3389/fphar.2013.00136

[43] Y. Shen, H. Zhang, S. Yao, F. Su, H. Wang, J. Yin, Y. Fang, L. Tan, K. Zhang, X. Fan, M. Zhong, Q. Zhou, J. He, Z. Zhang, *Clin. Transl. Med.* **2022**, *12*, e719. https://doi.org/10.1002/ctm2.719

[44] A. K. ElHady, S.-P. Shih, Y.-C. Chen, Y.-C. Liu, N. S. Ahmed, A. B. Keeton, G. A. Piazza, M. Engel, A. H. Abadi, M. Abdel-Halim, *Bioorg. Chem.* **2020**, *98*, 103742. https://doi.org/10.1016/j.bioorg.2020.103742

SUPPORTING INFORMATION

Additional supporting information can be found online in the Supporting Information section at the end of this article.

How to cite this article: H. G. Aboelfotouh, M. Abdallah, H. Khalifa, Y. Aboushady, A. H. Abadi, M. Engel, M. Abdel-Halim, *Arch. Pharm.* **2024**;*357*:e2400020. https://doi.org/10.1002/ardp.202400020